Rochester Institute of Technology
RIT Digital Institutional Repository

Theses

5-6-2019

Performing DNA ligation on a low-cost inkjet-printed digital microfluidic device

Sari Houchaimi
sxh4088@rit.edu

Follow this and additional works at: https://repository.rit.edu/theses

Recommended Citation
Houchaimi, Sari, "Performing DNA ligation on a low-cost inkjet-printed digital microfluidic device" (2019). Thesis. Rochester Institute of Technology. Accessed from

This Thesis is brought to you for free and open access by the RIT Libraries. For more information, please contact repository@rit.edu.

Performing DNA ligation on a low-cost inkjet-printed digital microfluidic device

By:

Sari Houchaimi

A thesis submitted in partial fulfillment of the requirements for the degree of Masters of Science in Mechanical Engineering

Department of Mechanical Engineering

Kate Gleason College of Engineering

Rochester Institute of Technology

Rochester, New York

Submitted on 05/06/2019

Performing DNA ligation on a low-cost inkjet-printed digital microfluidic device

By:

Sari Houchaimi

A thesis submitted in partial fulfillment of the requirements for the degree of Masters of Science in Mechanical Engineering

Department of Mechanical Engineering

Kate Gleason College of Engineering

Approved by:

Dr. Michael J. Schertzer, Assistant Professor *Thesis Advisor, Department of Mechanical Engineering*	Date
Dr. Patricia Iglesias Victoria, Assistant Professor *Committee Member, Department of Mechanical Engineering*	Date
Dr. Kathleen Lamkin-Kennard, Associate Professor *Committee Member, Department of Mechanical Engineering*	Date
Dr. Michael G. Schrlau, Associate Professor *Department Representative, Department of Mechanical Engineering*	Date

ABSTRACT

DNA Synthesis is a critical component in many biological and medical applications. Unfortunately, the production of DNA is tedious, time consuming, and expensive. To accelerate the production times and lower the cost, we take a closer look at the potential application of digital microfluidics for this process.

Microfluidics involves manipulating small volumes of fluid (microliters). It takes advantage of the relative dominance of forces such as surface tension and capillary forces at the submillimeter scale. This allows for lower reagent consumption and shorter reaction times. The technology is also portable and can accommodate for various functions to be performed on the device itself. A particularly appealing focus of this field is Digital Microfluidics (DMF).

Digital Microfluidics (DMF) is a relatively recent technology praised for its fast analysis times and small volume requirements (microliters). An obstacle to the production of DNA chains using traditional methods of nucleotide synthesis is the requirement of acetonitrile, which can't consistently be manipulated on DMF. Another obstacle to overcome is the accurate production of long chains of nucleic acids (3000 to 5000 base pair products), much longer than the DNA products used in a typical ELISA assay. For the sake of this project we are partnering with Nuclera Nucleics, a company based in the United Kingdom working on a next-generation DNA synthesis and automation platform. The company has created a novel way of synthesizing DNA using aqueous chemistry. Collaborating with them, we propose to build a DMF device that will perform oligonucleotide synthesis. The first step towards this goal is to verify that DNA ligation can be executed on a DMF device.

This device will make DNA synthesis more accessible and significantly reduce production times in the laboratory. This will lead to more advancements in the field of genetics, drug delivery and other biomedical applications.

ACKNOWLEGMENTS

I would first like to thank my Faculty Advisor, Dr. Michael J. Schertzer, for giving me the opportunity to work on a potentially groundbreaking technology. His knowledge, patience and unending support allowed me to steer my research in the right direction. His door was always open when I had doubts or needed guidance.

I would also like to thank Dr. Michel from the College of Science, as the biological procedures in this study would have not been performed without her help.

I would also like to thank Nuclera for giving me the opportunity and resources to work with them on a project that may revolutionize DNA synthesis.

I must also express my sincere gratitude to my Graduate Director, Dr. Michael Schrlau, who allowed me to carry out my research, guided and motivated me throughout the way.

I am extremely grateful for my colleagues, Collin Burkhart, Kimberly Bernetski, Hee Tae An and Xi Li, for sharing their knowledge and contributing to my research. Completing this research would have been much harder without their support.

I also extend my gratitude to all the professors in the Mechanical Engineering department and the College of Science for enriching my knowledge during my time at RIT.

Finally, I would like to thank my parents for encouraging and supporting me throughout this journey.

TABLE OF CONTENTS

LIST OF FIGURES

LIST OF TABLES

LIST OF APPENDICES

NOMENCLATURE

Symbol	Meaning
a	Radius of spherical particle
C	Capacitance per unit area (F/m^2)
DEP	Dielectrophoresis
DMF	Digital Microfluidics
DNA	Deoxyribonucleic Acid
$\vec{E}$	Electric Field (N/C)
ELISA	Enznyme-Linked ImmunoSorbed Assay
EWOD	Electrowetting On Dielectric
f_{CM}	Clausius-Mossotti Factor
FIA	Fluorescent Immunoassay
HRP	Horseradish Peroxidase
IJP	InkJet-Printed
ITO	Indium Tin Oxide
$\vec{p}$	Dipole Moment Vector (C.m)
PCI	Peripheral Component Interconnect
PCR	Polymerase Chain Reaction
PDMS	Polydimethylsiloxane
PFC	Perfluorinated Chemicals
PXI	PCI Extention for Instrumentation
RNA	Ribonucleic Acid

V	Voltage (V)
γ_{SL}	Solid-Liquid Interfacial Tension (N/m)
γ_{SLD}	Interfacial Tension when there is no voltage (N/m)
γ_{SG}	Solid-Gas Interfacial Tension (N/m)
γ_{LG}	Liquid-Gas Interfacial Tension (N/m)
θ_0	Contact Angle without voltage applied (°)
θ	Contact Angle with voltage applied (°)
ε_m	Relative Permittivity of suspending medium (F/m)
ε_p^*	Complex Permittivity of particle (F/m)
ε_m^*	Complex Permittivity of suspending medium (F/m)

1.0 INTRODUCTION

1.1 Background

Solid phase DNA synthesis is one of the most important protocols in health care and medical research [1]. The accurate production of long chains of nucleic acids (3000 to 5000 base pairs) requires long labor hours and is expensive, as laboratories still rely on the same traditional methods of producing them [2, 3]. These chains can be employed to probe genomic libraries for unique DNA sequences, or to engineer changes in a protein structure [4]. This creates a practical bottle neck in a variety of critical applications, including gene expression profiling, genome annotation and directed mutagenesis [2, 4]. It would therefore be beneficial to produce DNA rapidly and at low cost. The work presented here was performed in partnership with Nuclera Nucleics who have created a novel chemical method to accurately perform oligonucleotide synthesis using aqueous chemistry. Since this process employs water in lieu of acetonitrile, the advantages of digital microfluidic automation can be used to increase throughput of oligonucleotides.

Microfluidics is the field involving the manipulation of fluids at the submillimeter scale. At this scale, the relative importance of physical forces changes. Forces like surface tension and capillary forces become dominant. It is an attractive technology since it leads to shorter reaction times and lower reagent requirements, as well as portability and multifunctionality on one small platform. An interesting focus of this field for the application of DNA synthesis is Digital Microfluidics (DMF). Digital Microfluidics (DMF) consists of manipulating discrete droplets of liquid by actuating electrodes contingent to them on the device (Figure 1.1). It is a portable technology that provides results quickly and only requires small volume samples, as all droplet

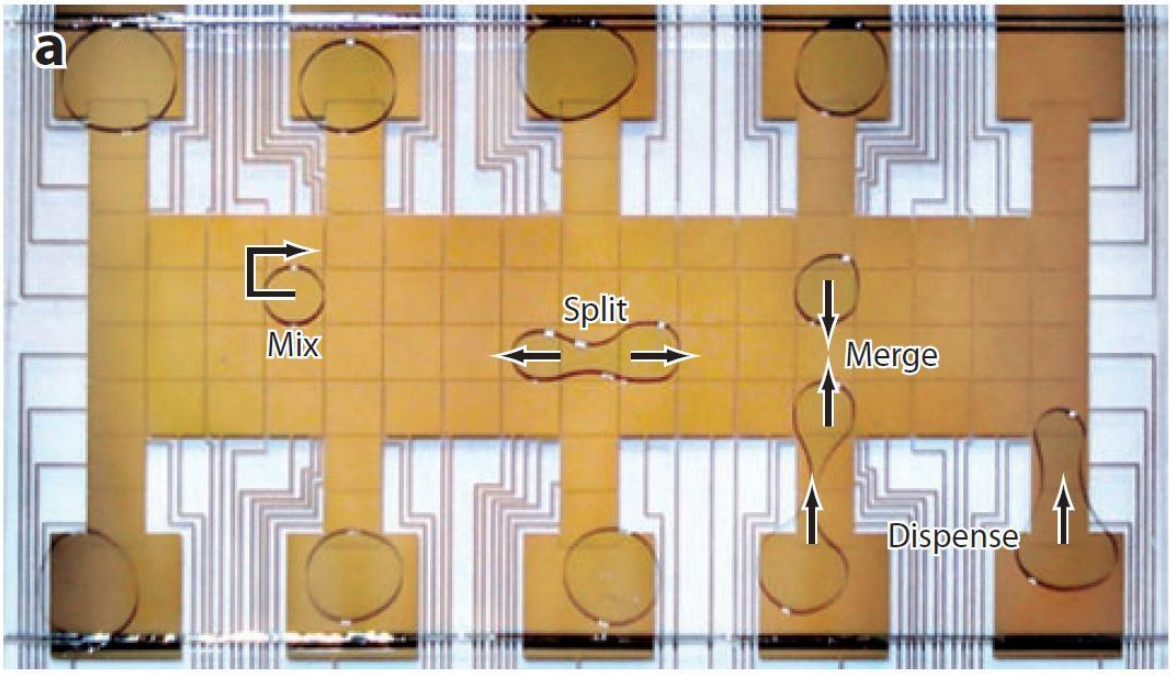

Figure 1.1*:* Image of a DMF device with droplet operations performed: (i) dispensing, (ii) merging, (iii) splitting, (iv) and mixing of microliter-sized droplets [26]

operations can be done on the DMF device directly [5]. It is also reprogrammable to suit the procedure needed and can handle multiple reagents without increasing the fabrication complexity of the device. It could be used to automate complex biological protocols like oligonucleotide synthesis. DMF devices have not been used to automate solid phase oligonucleotide synthesis because it typically requires the use of acetonitrile at high concentrations for higher yields [6], which can only be manipulated consistently on DMF at low concentrations [7].

The first step towards achieving the goal of this partnership with Nuclera is to develop a DMF device that allows for DNA ligation on its surface without adversely affecting it. This is verified by merging and mixing droplets containing two separate bricks of DNA provided by the industrial partner in two different settings. This experiment is first executed on the bench top using an Eppendorf tube in order to get a reference for our next results, then on the digital

microfluidic device by employing its droplet operation capabilities (dispensing, merging and mixing). A DNA gel electrophoresis is then run, separately evaluating the weight of the ligated bricks on bench and the ligated bricks on the digital microfluidic device. To confirm the success of this experiment, the DNA bricks ligated on the bench and those ligated on the device will need to have a similar electrophoretic migration, i.e. the same number of base pairs.

1.2 Literature Review

Oligonucleotide Synthesis

Oligonucleotide synthesis allows for the chemical production of long chains of nucleic acids. The most proficient process to produce oligonucleotide is through the use of phosphoramidite monomers [8]. A phosphoramidite monomer is a nucleotide surrounded by protection groups: trityl, amine, hydroxyl and phosphate groups (figure 1.2). These protection groups ensure the formation of the desired product and inhibit any fouling or side reactions. There are four main stages in the synthesis cycle: deprotection, coupling, capping and oxidation. The first step of DNA synthesis is deprotection. The trityl group is removed by trichloroacetic acid, leaving a hydroxyl group to react with the next base added. The second step is coupling. Tetrazole is employed to increase coupling efficiency. It is a weak acid that attacks the phosphoramidite nucleoside to form a tetrazolyl phosphoramidite intermediate. The latter will react with the hydroxyl group left after deprotection. The next step is capping. An acetylating reagent composed of acetic anhydride and N-methylimidazole is added. This reagent essentially gets rid of coupling failures by irreversibly capping the oligonucleotides concerned. The last step is stabilization. Water and Iodine are added. This leads to the oxidation of the phosphide into phosphate, stabilizing the bond. The steps are then repeated for each nucleotide (figure 1.3).

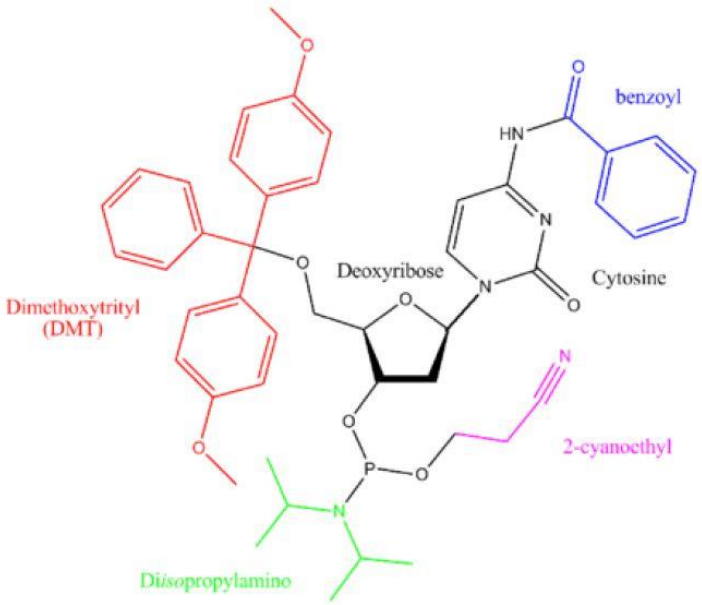

Figure 1.2: Protection groups in a phosphoramidite monomer [8]

Oligonucleotide synthesis is an important process for a variety of biological and medical applications [9]. It is employed as primer for DNA sequencing or amplification, antisense oligonucleotides, and interfering RNA [8]. Each oligonucleotide is custom made to fit the needs of a specific research procedure [8]. Oligonucleotide synthesis is also crucial in the study of heritable gene regulation (epigenetics) [9]. It can allow further cataloging of genome-wide DNA methylation patterns, which shows specific modifications of the function and expression of genes [10]. Unfortunately, there are still obstacles to overcome with Oligonucleotide synthesis. It typically requires long hours of preparation and manipulation in laboratories [11]. One of the major cost problems is the inability to lower the reagent consumption and reduce material waste without in turn affecting the yields, making it very expensive to produce oligonucleotides [2]. Nuclera Nucleics proposes a protocol for accurately producing long DNA chains using highly engineered enzymes, discussed further in section 3.3.

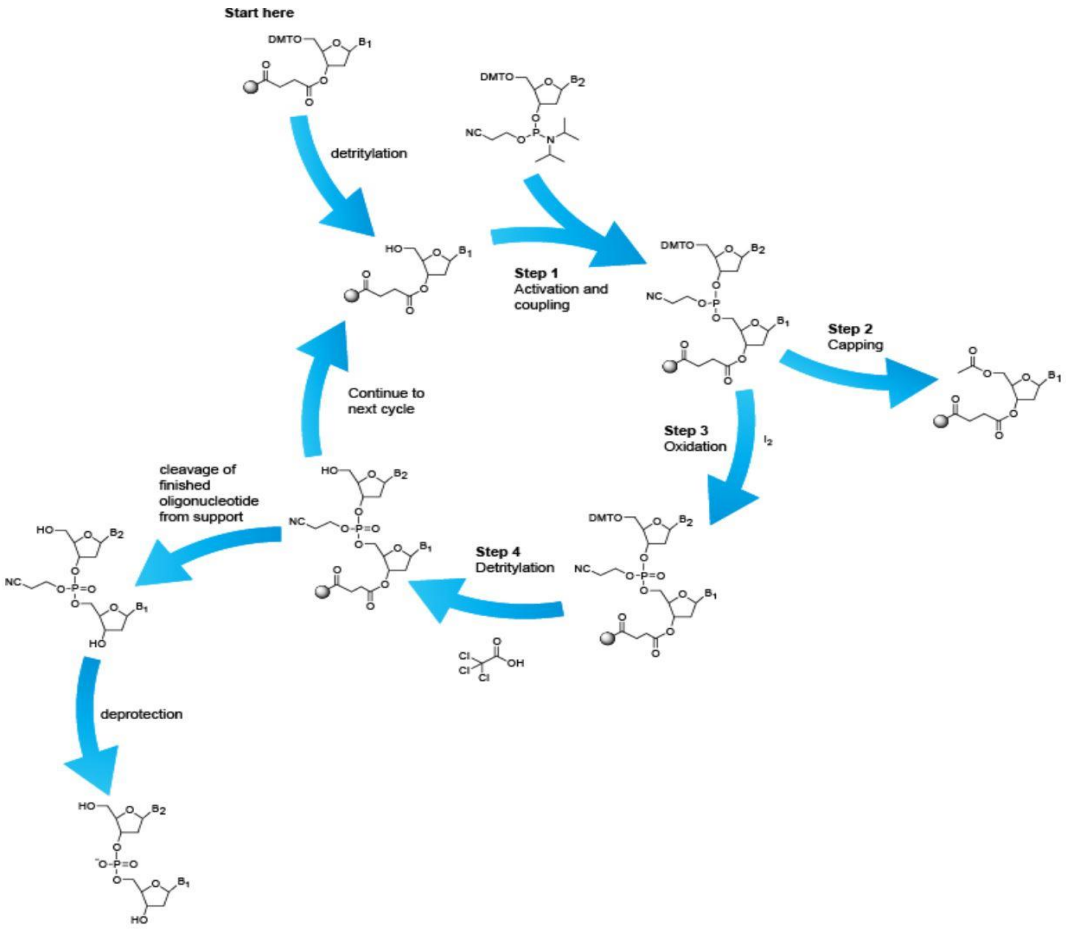

Figure 1.3: Oligonucleotide synthesis using phosphonamidite, established as the method of choice [40]

DNA ligation is the process of joining two linear fragments of DNA with covalent bonds (figure 1.4). A ligase is employed as a catalyzer to help form covalent bonds and repair breaks in nucleic acid chains. It is an essential process in gene applications such as gene cloning and DNA or RNA synthesis [12].

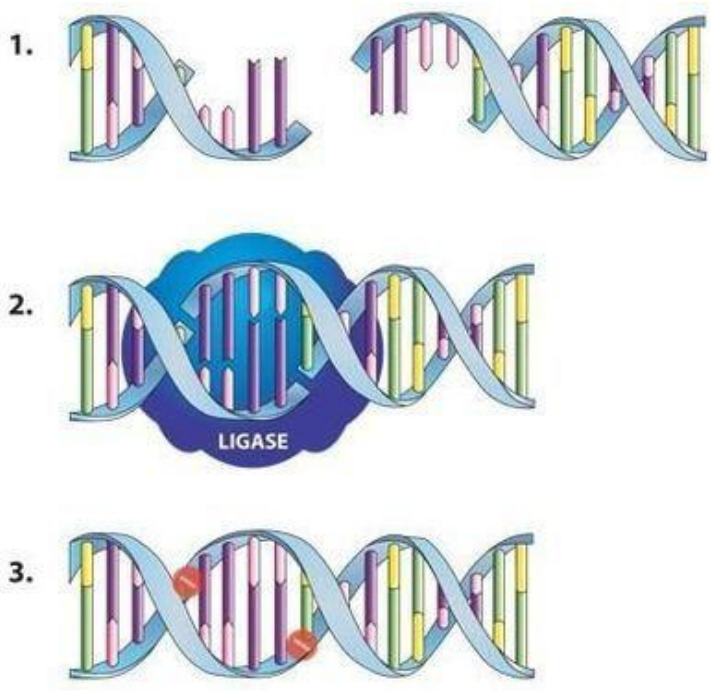

Figure 1.4: Traditional DNA ligation process: (1) Two bricks of DNA on left and right, (2) Ligase introduced to form covalent bonds between the two DNA fragments, and (3) The two DNA fragments are now merged into one bigger DNA brick [41]

The ligation process is typically done in vitro using commercial DNA kits that require a large sample volume (~15µL), and can take up to several hours of labor to complete. The commercial kits available are expensive and can only synthesize up to 1000 base pairs [10], so there is currently no commercial solution to fulfill the needs of laboratories looking to work with longer oligonucleotide chains. Scientists have to purchase separate chains and assemble them themselves to achieve the number of base pairs required. It has been reported that the standard procedures result in a waste of 85% of the DNA and enzyme/buffer volume (figure 1.5) [13]. A potential solution to these issues would be to apply the concept of microfluidics, specifically digital microfluidics, to oligonucleotide synthesis.

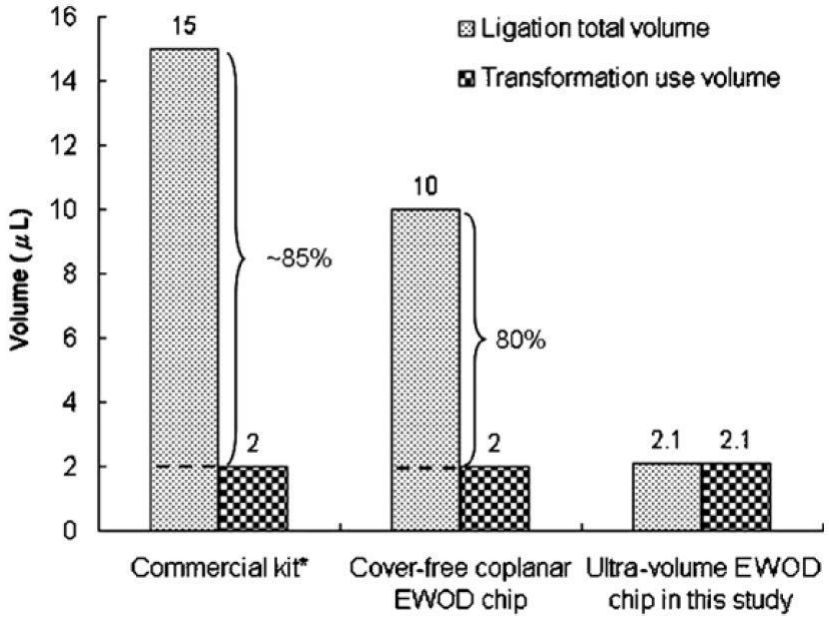

Figure 1.5 : Comparison of the volume of reagent usage for transformation in three operating methods [13]

Digital microfluidics

The domain of microfluidics concerns the manipulation of fluids at the submillimeter length scale. It is an attractive technology as the small size and automatability of microfluidic devices provide advantages like shorter reaction times, low reagent requirement and function variety on a standalone platform [14]. It eliminates the usual expensive bench top biomedical devices needed to conduct a simple clinical test. It allows for faster analysis, portability, and small volume samples, as operations are done directly on the microfluidic device [5]. It is also versatile and reprogrammable to suit the assessment needed. It is particularly appealing as the relative importance of different forces change when nearing microscale. Indeed, the surface

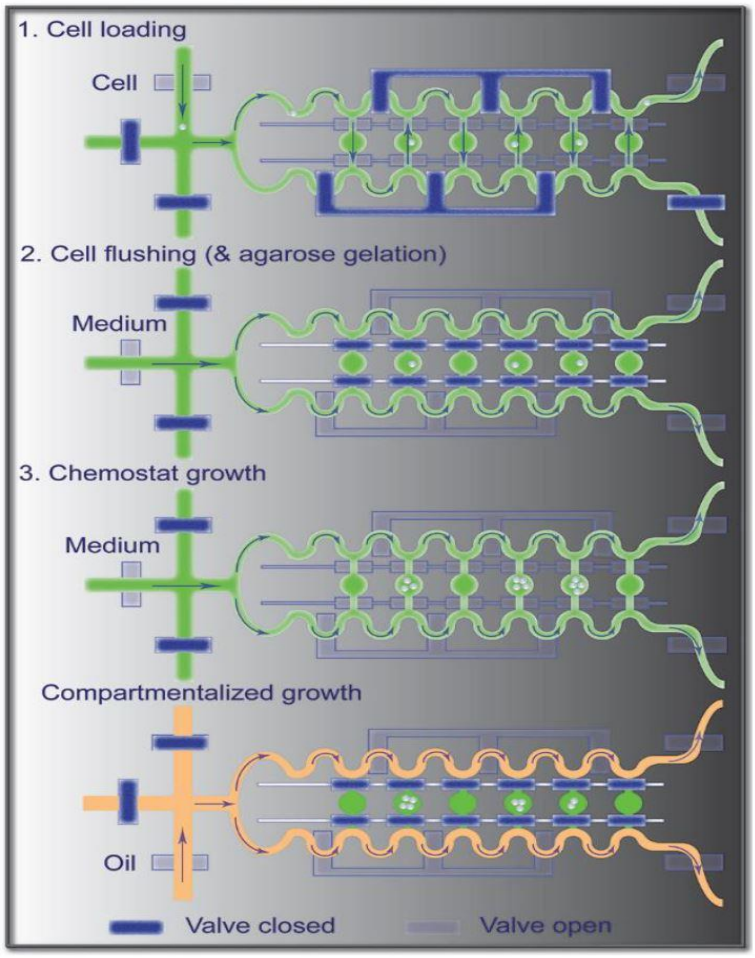

Figure 1.6: Microchannel based microfluidic device for cell culture: (1) Cells are loaded into the device and flowing through the growth chambers in the middle, (2) Fresh media is infused with the growth chamber valves (isolation valves) closed to flush out any cells remaining in the channels, (3) chemostat conditions created by flowing media with the isolation valves open vs compartmentalized growth where isolation valves are closed and oil is infused into the main channels [17]

tension and capillary forces become dominant at the microscale. This opens the door for a myriad of applications with high analytical throughput [15]. As such, it is possible to passively pump fluids in microchannels without the use of an actual pump [16]. It also presents potential solutions for point of care testing, medical diagnostics, and biology research. Microfluidic devices can also be used to mimic conditions for cell culture, controlling the environment of

those cells directly in the device [17] (figure 1.6). In drug delivery for instance, microsystems equipped with sensors are capable of delivering precise drug doses [18]. Integrated chemical analyzers may be used to analyze a whole blood sample of only 1μL for HIV and syphilis in a matter of minutes instead of hours [19]. Microfluidics are also employed to detect a known prostate cancer biological marker, Prostate Specific Antigen (PSA) [20]. An interesting emerging field is Digital Microfluidics (DMF), which allows active fluid handling of individual droplets over an array of electrodes.

Digital Microfluidics (DMF) is a relatively recent microfluidic platform that manipulates individual droplets of fluid using electric fields. DMF devices consist of droplets of liquid above an array of electrodes coated with a dielectric and hydrophobic layers [5, 24–26]. As opposed to the passive use of capillarity in microchannels [19, 20](Figure 1.6), droplets are manipulated by electrowetting on dielectric (EWOD). Electrodes contingent to the droplet are actuated to displace it. The electric field created will change the interfacial energy between the droplet and the surface, reducing the contact angle and "wetting" the surface [25, 27] (Figure 1.7).

The physics of electrowetting help understand the operation of a DMF device. Berge combined Lippmann's law (equation 1) with Young's equation (equation 2) to relate the contact angle and the electric potential, leading to the Lippmann-Young equation (equation 3) [25]:

$$\gamma_{SL} = \gamma_{SDL} - \frac{c}{2}V^2 \quad (1)$$

γ_{SL} is the solid-liquid interfacial tension when the voltage is applied, and γ_{SLD} is the interfacial tension when there is no voltage. C is the capacitance per unit area of the dielectric layer covering the electrodes in the DMF device, and V is the voltage applied.

$$\gamma_{SL} = \gamma_{SG} - \gamma_{LG} \cos\theta \tag{2}$$

$$\cos\theta = \cos\theta_0 - \frac{1}{\gamma_{LG}} \frac{1}{2} CV^2 \tag{3}$$

In the above equations, γ_{SG} is the solid-gas interfacial tension, γ_{LG} is the liquid-gas interfacial tension and θ_0 and θ are the contact angles without and with the voltage applied, respectively. When applying the voltage to the adjacent electrode, charges in the droplet gather at the liquid-solid-gas interface. This leads to a decrease of the liquid-solid interfacial tension. The driving force is the result of electrostatic forces varying the apparent wettability of the system [26].

DMF devices reduce diffusion times by automating the process with simple and compact equipment, and reducing reagent consumption overall [27]. This leads to faster analysis and lower cost. The liquid can be surrounded by a carrier oil (e.g. silicone oil) [28], or by air [29]. As such, DMF is an attractive candidate for clinical applications on biomedical devices, especially point of care testing and immunoassays [5]. DMF enables each droplet to be controlled individually, without the need for physical elements such as valves or mechanical mixers [26].

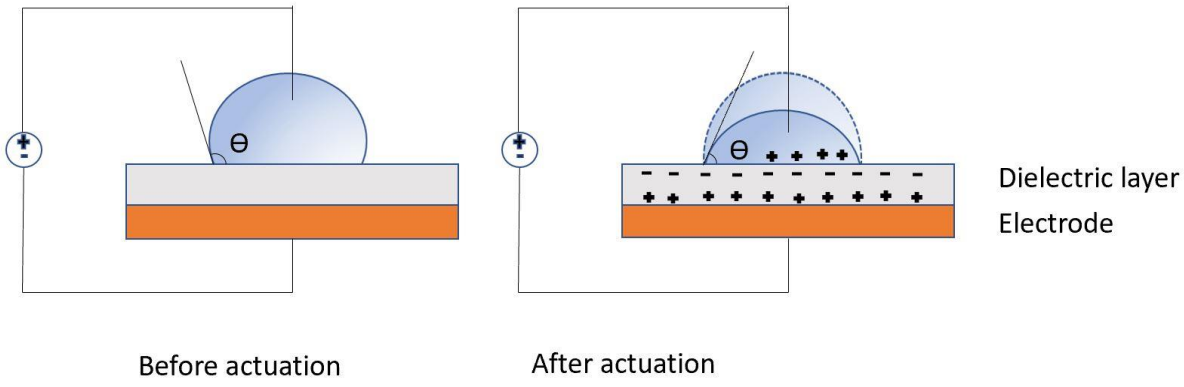

Figure 1.7: EWOD with effect on contact angle in an open device (left), and a general structure of a closed DMF device (right)

A final point worth noting is that the fabrication of DMF devices can be slow and expensive. It generally requires cleanroom facilities for microfabrication [24]. Recently, low-cost inkjet fabrication methods have been used to create DMF devices with similar performance to cleanroom fabricated devices. Using a consumer-grade inkjet printer, a paper with electrodes can be printed using metallic ink. The device is assembled using glass slides, and the upper and lower plates are coated with layers of Teflon, ITO and PFC [30]. This makes inkjet-printing of DMF devices an attractive method for rapid prototyping as it effectively reduces costs and time compared to cleanroom fabrication methods [31]. This study takes a closer look at operations on inkjet-printed microfluidic devices, as this allows several designs to be manufactured and tested out in a shorter time than the cleanroom fabricated ones.

1.3 Contributions

DNA synthesis is a bottleneck in many biological research applications and medical diagnostics. The current methods of synthesizing DNA are costly and time consuming. It would therefore be beneficial to figure out a way to synthesize DNA quickly and cheaply. The application of digital microfluidics to automate this process on a portable device gives rise to the possibility of achieving accurate results in a shorter amount of time. It also allows for the significant reduction of reagents consumption since only microliter droplets are used. Partnering with Nuclera Nucleics, we proposed to build a DMF device that would be able to perform oligonucleotide synthesis using aqueous chemistry instead of the use of acetonitrile, previously never executed. By performing DNA ligation on a DMF device, this demonstrates that DNA synthesis is possible on a DMF device using Nuclera's chemical process. This will open the doors for a more accessible means of producing DNA, thus paving way for further innovations in medical and biological applications.

2.0 RESEARCH QUESTION

The primary goal of this thesis is to answer the following question: **can DNA ligation be executed on a digital microfluidic device using Nuclera's novel aqueous protocol?** DMF DNA ligation will be benchmarked against the bench top biochemical process following a protocol provided by Nuclera. Thus, if successful on a digital microfluidic device, this protocol could revolutionize the way we synthesize DNA, as it provides a cheaper and faster way of doing so. This study is just the first step towards achieving an automated DMF platform for oligonucleotide synthesis.

All the operations performed were performed on inkjet-printed digital microfluidic devices, while another student in the DMFL (Hee Tae An) performed the same process on cleanroom fabricated DMF devices. A secondary goal of this work is to **determine if low-cost IJP devices can provide similar results as cleanroom devices.** These inkjet-printed DMF devices are more accessible as they are easier to fabricate, and do not require any expensive equipment for manufacturing: no chemical process is involved such as etching or chemical deposition, and no precautions have to be taken (cleanroom attire). The low-cost DMF devices can be built in the DMFL directly using common equipment such as a printer and glass slides.

3.0 EXPERIMENTAL METHODOLOGY

This section is broken down into three major categories: device fabrication, device operation, and experimental analysis. The device fabrication section will mainly comprise of the device manufacturing procedures and the evolution of the designs adopted over time. The device operation section will explain the experimental design along with the protocol employed for DNA ligation on and off the device and the droplet composition. The experimental analysis will discuss the process and equipment for running the gel electrophoresis in order to evaluate the DNA migration.

3.1 Device Fabrication

A DMF device generally consists of two substrates, a conductive layer, hydrophobic and dielectric layers. The breakdown of the components for both bottom and upper part of a DMF device is as follows:

- Bottom plate:
    - Substrate
    - Conductive layer
    - Dielectric Layer
    - Hydrophobic layer
    - Spacer
- Top plate:
    - Substrate
    - Conductive layer
    - Hydrophobic layer

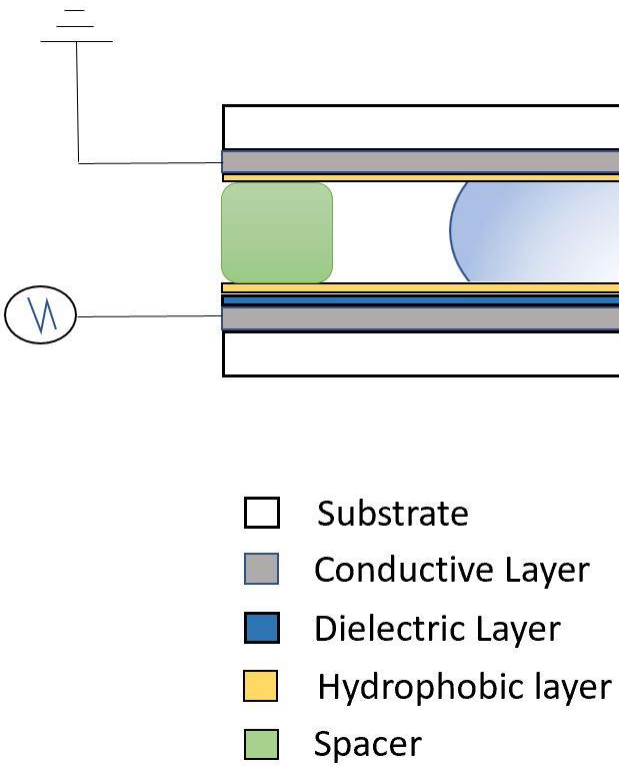

Figure 3.1: General structure of a DMF device

The hydrophobic and dielectric layers on the bottom part of our devices were spin coated in the following order:

1- 6% Teflon Layer (hydrophobic layer ~100nm thick) (figure 3.3)
2- SU-8 Layer (dielectric layer ~4.4μm thick) (figure 3.4)
3- 6% Teflon Layer (hydrophobic layer ~100nm thick) (figure 3.5)

A first hydrophobic layer of Teflon was necessary as the SU8 film did not bond well to the printing media [32]. Kapton tape was used to stick the printing media on the glass slide once the electrodes were printed and dried at room temperature for 24 hours. The bond pads were also covered with Kapton tape, and were removed after the spin coating is done. This keeps the bond pads exposed to be able to actuate the corresponding electrodes.

The top part of the device will also feature the glass slide (50x25mm) substrate coated with ITO, directly procured from Delta technologies (Surplus part # X172). A layer of Teflon is spin coated on top of the ITO layer (figure 3.2). A small patch was scratched off after coating in order to ground the device by using a piece of copper tape linked to the ITO layer. During the assembly of the top and bottom parts of the device, double sided tape of approximately 100µm thickness was employed as spacers (figure 3.6).

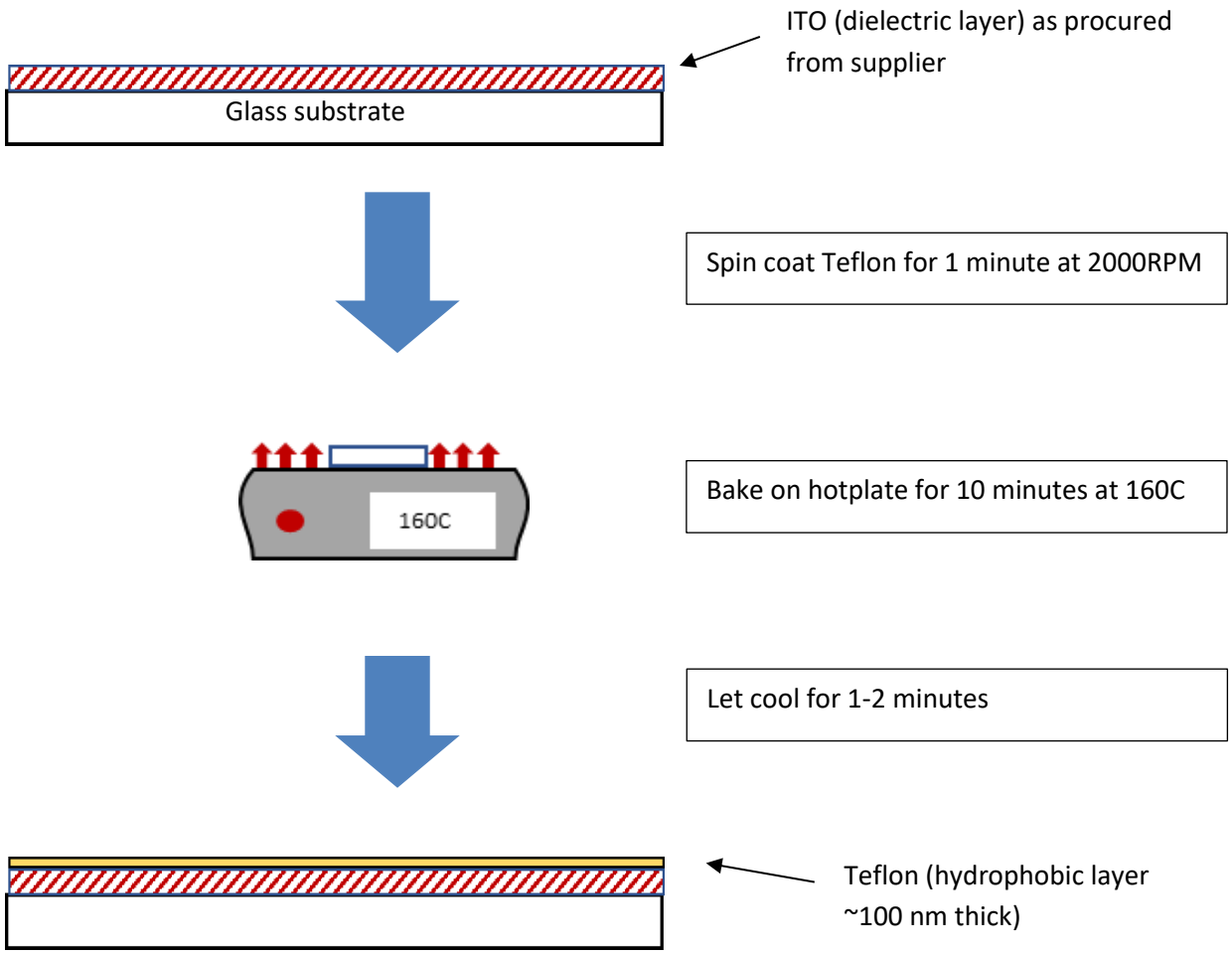

Figure 3.2: DMF device top plate fabrication flow chart

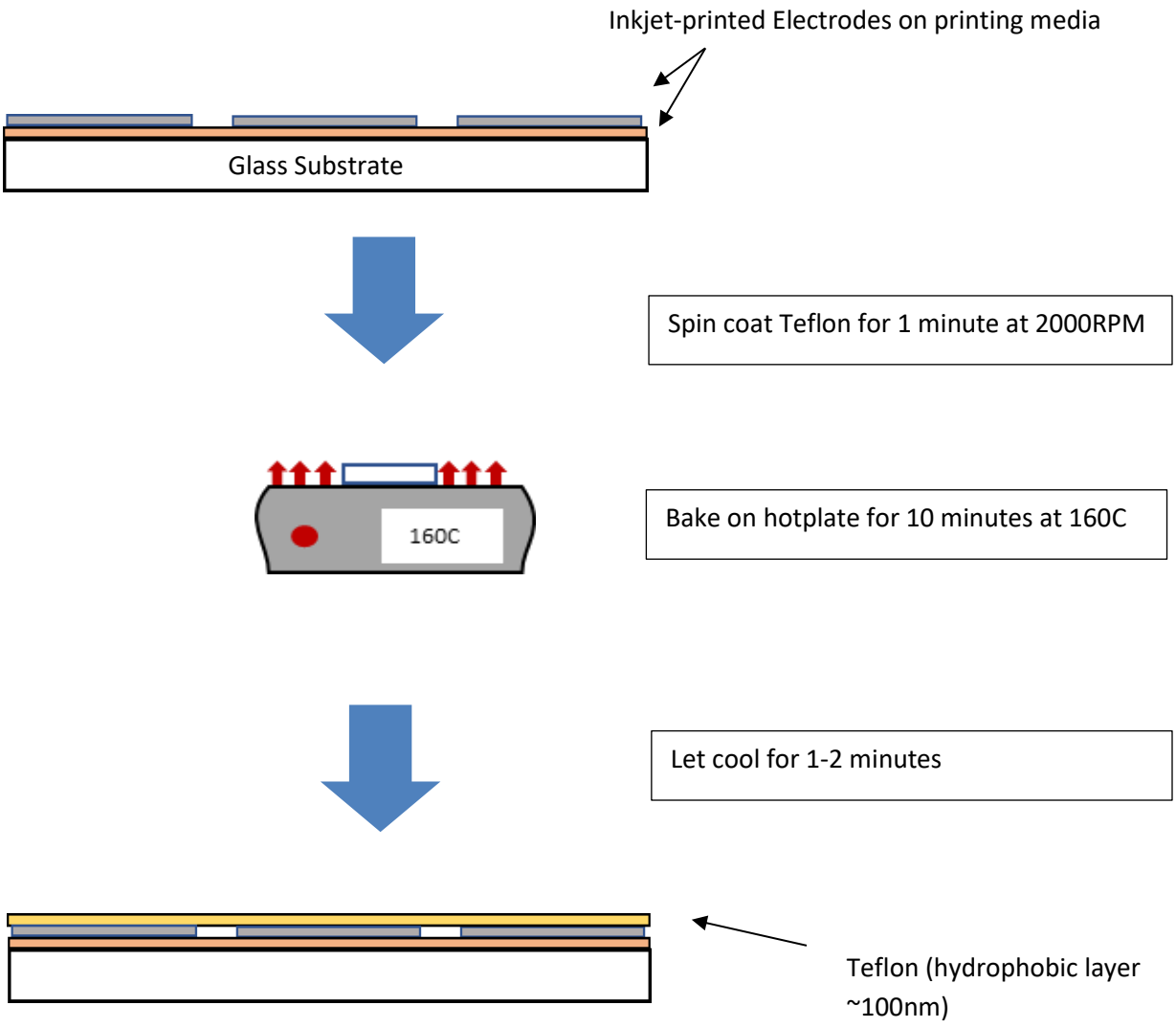

Figure 3.3: DMF bottom plate fabrication flow chart part 1 (first hydrophobic layer)

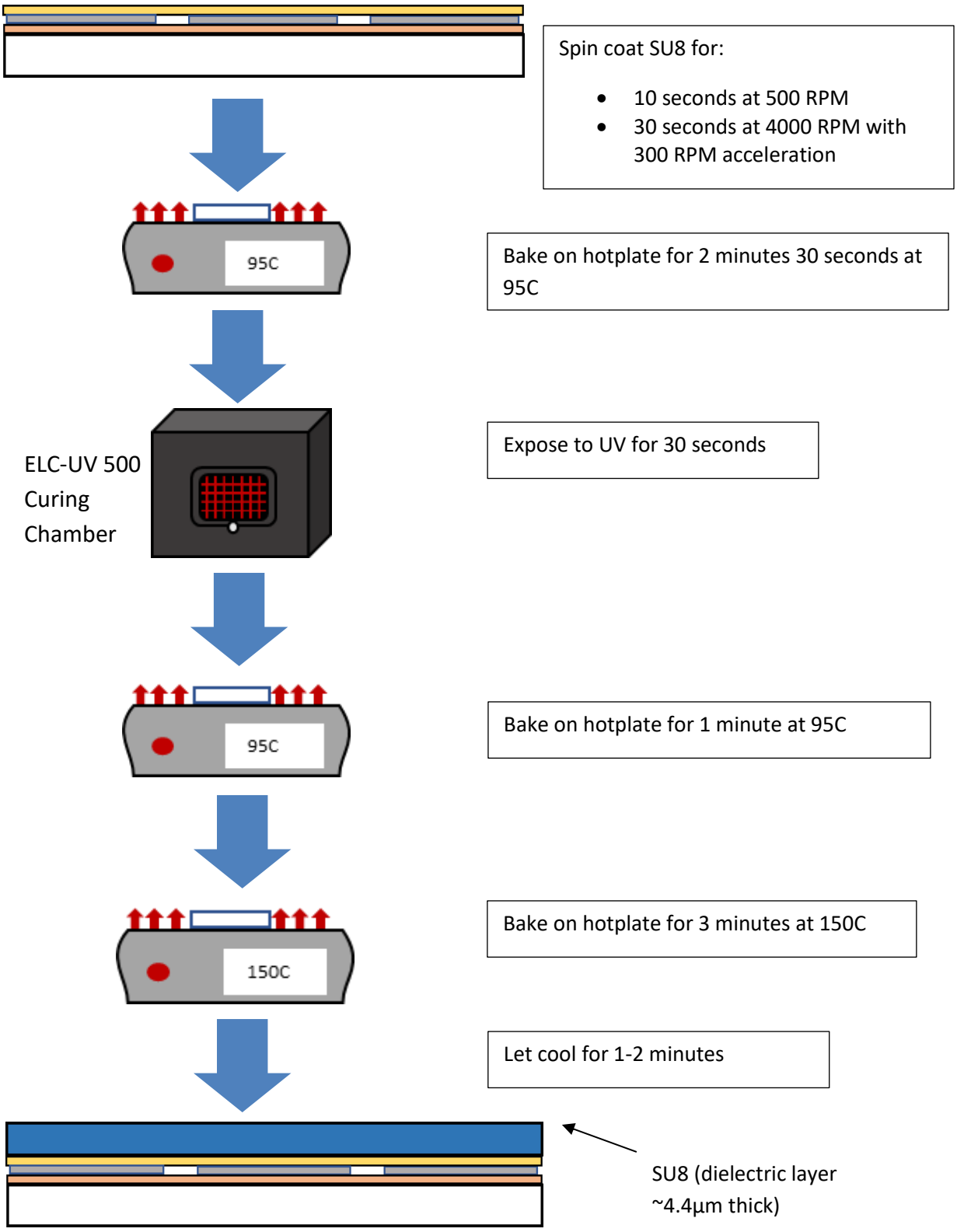

Figure 3.4: DMF bottom plate fabrication part 2 (dielectric layer)

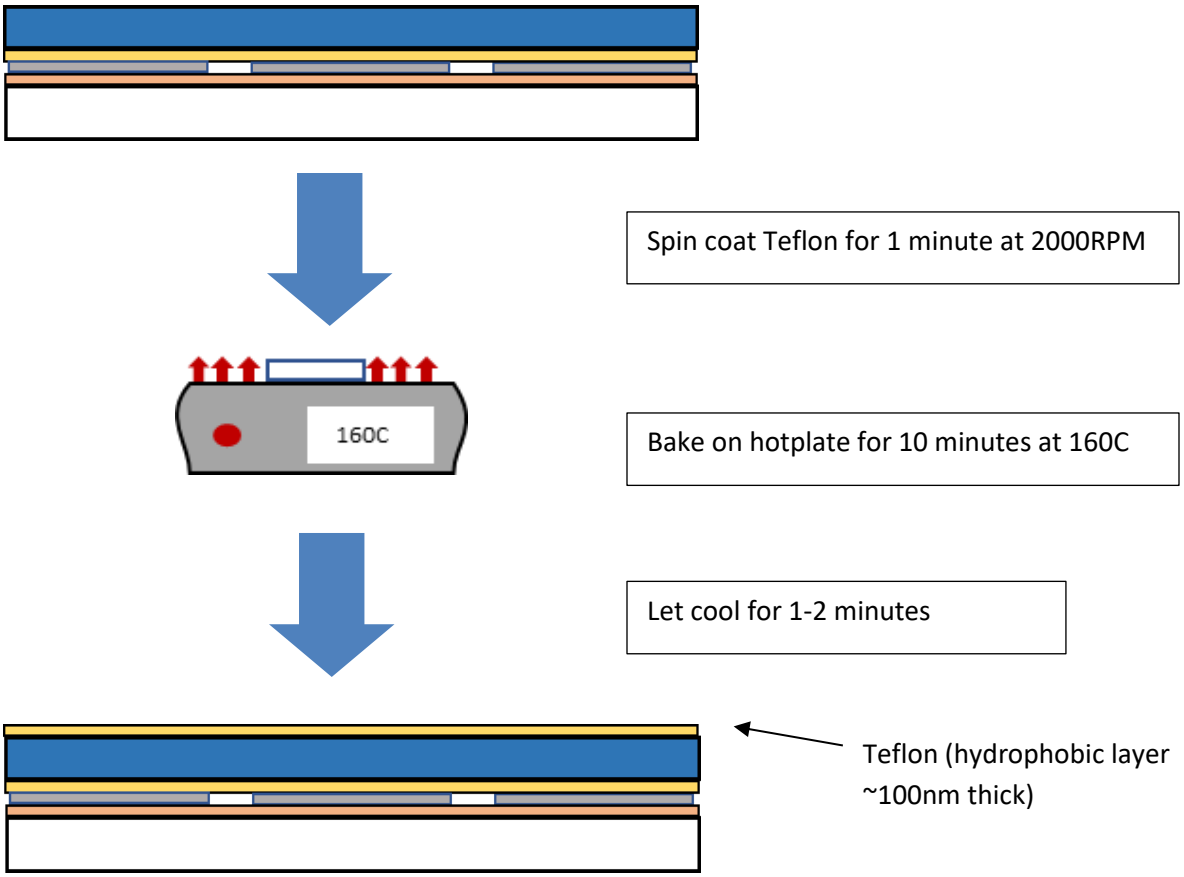

Figure 3.5: DMF bottom plate fabrication flow chart part 3 (second hydrophobic layer)

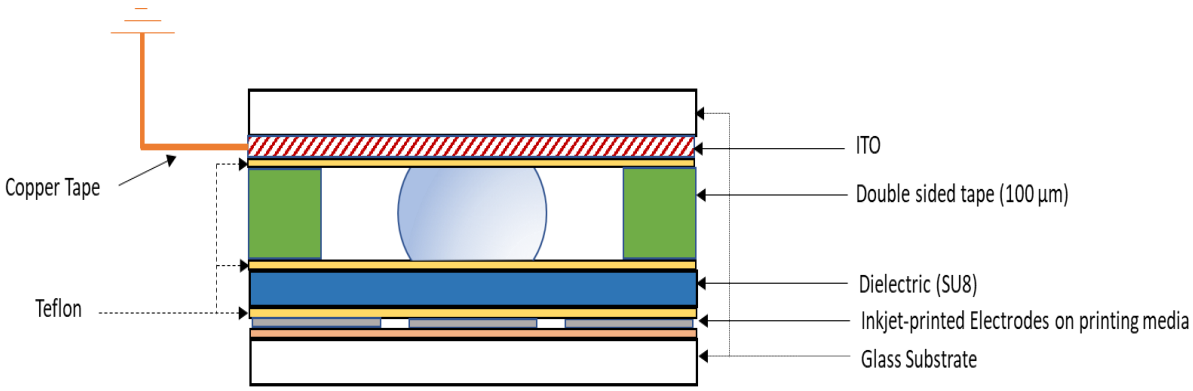

Figure 3.6: DMF device after assembly of top and bottom parts

This fabrication process is faster than the conventional cleanroom fabrication procedure used by my DMFL colleague Hee Tae. Indeed, cleanroom fabrication involves steps using several equipment in order to first etch the substrates, then sputter the electrodes (Aluminum), perform a first level lithography to develop the substrates, then etch the sputtered electrodes, dice the substrate, then perform a second level lithography to develop the dielectric layer and finally spincoat the hydrophobic layer. This process can take several hours to several days due to the scheduling of the equipment. This compares to using only an inkjet-printer, a spincoater and a UV cure chamber outside the cleanroom for manufacturing IJP devices. Also, the IJP devices only require nitrile gloves for handling as the fabrication is done directly in the DMFL whereas the cleanroom has strict precaution and protection guidelines (protective equipment).

Electrodes were designed in Adobe Illustrator. The primary design comprised of two reservoirs and six transport electrodes only. For the first try, a simple layout has been chosen to facilitate testing and observations. The first print with three separate electrode designs had very spaced out electrodes (0.75mm) to get familiar with the process. A set of these three designs with 0.75mm spacing was created and printed (figure 3.7). The reservoirs provide the supply to create a droplet on the DMF device. A C-shape reservoir was mainly adopted. An L-shape was also created to compare the ease of droplet creation on the device. Continuity between the electrodes was checked using a multimeter to determine whether electrodes were shorted.

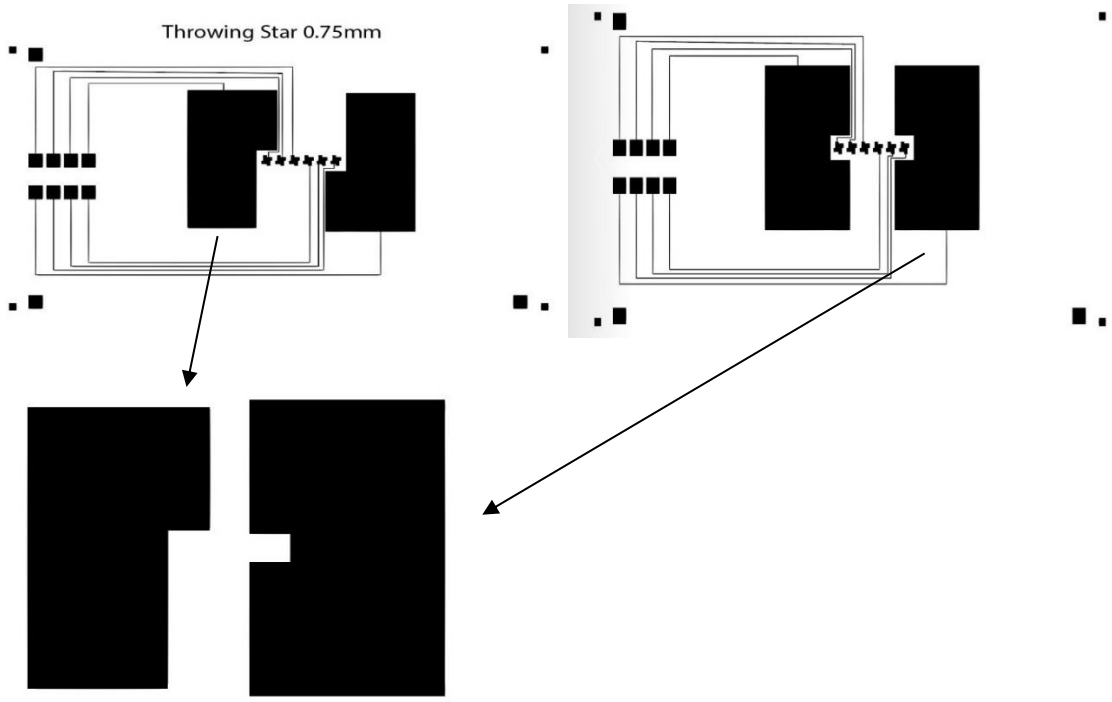

Figure 3.7: L-shape vs C-shape reservoirs close-up

The minimum spacing between all elements on the IJP electrodes was chosen from literature to be at least 0.15mm, or 150μm, to keep the printed patterns loyal to the ones designed and to reduce the probability of shorts happening between electrodes [30]. Two different shapes of transport electrodes were drawn: square and star shaped electrodes inspired by multiple works from the Wheeler Microfluidics Laboratory [7, 26, 32] . A set of z-block electrode designs was initially drawn and printed as well (figure 3.8), but was dropped for the next iteration.

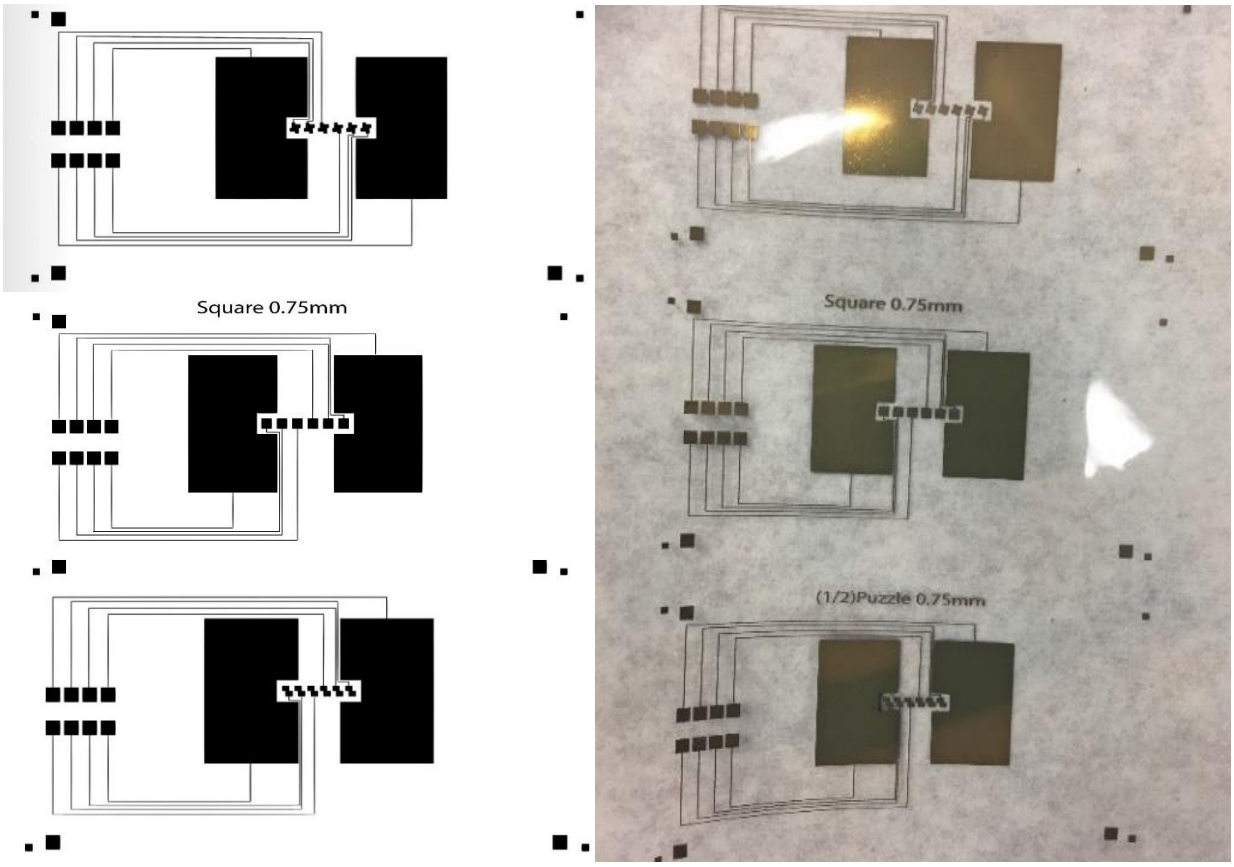

Figure 3.8: 3 designs before printing (left): star (top), square (middle), and z-block (bottom), and after printing (right)

The electrodes were printed using an Epson C88+ Stylus printer (figure 3.9) with Novacentrix JS-B25P silver ink with particle size 83 nm, on a Novacentrix Novele printing media, a PET based substrate with porous coating. The printer settings were the following:

- Paper type: premium glossy photo paper
- Print quality: Best
- Image type: Line art

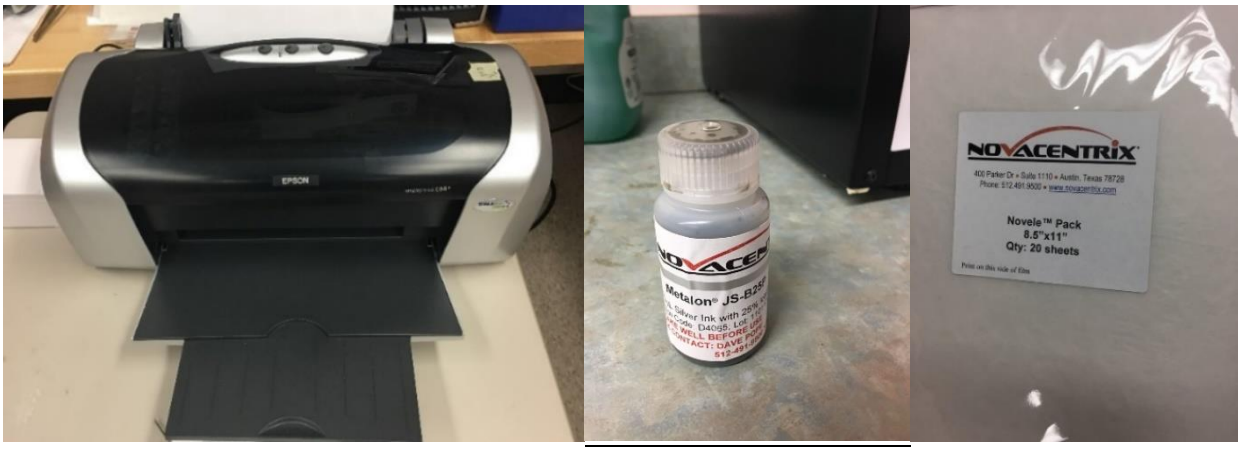

Figure 3.9: Pictures of Epson C88+ Printer (left), the silver ink (middle) and the polymer printing media used (right).

The next IJP electrodes printed had an electrode gap of 200µm (figure 3.10). The smaller distance helped execute droplet movement but was limited by the printer resolution. Printed electrodes were reported in literature to be closer than the distance initially set on the design, while the traces linking the electrodes to the bond pads are reported to be thicker than drawn [30]. The reservoir electrodes were 20mm by 12mm roughly, and the transport electrodes were 1.5mm by1.5mm, while the traces were drawn 150µm thick.

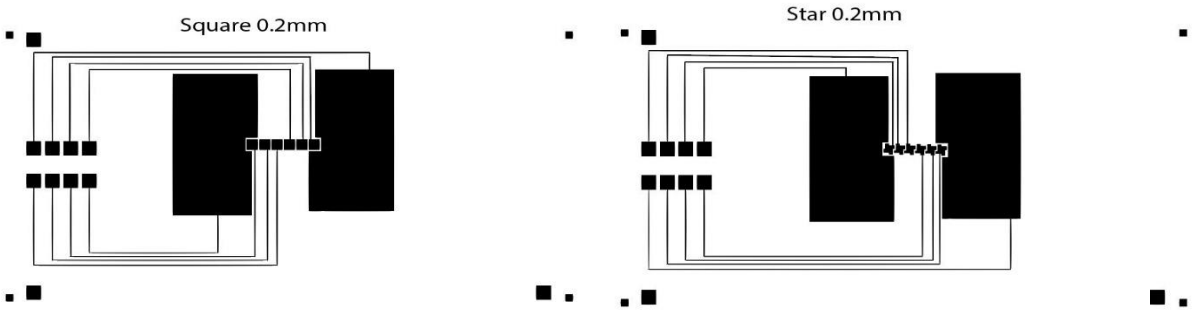

Figure 3.10: Electrodes printed with 200µm spacing between square electrodes (left) and between star electrodes (right)

Difficulties with droplet splitting from the reservoir were encountered with this design, as the reservoir electrode was deemed too big compared to the transport electrode (figure 3.11). The size of the reservoir directly affects the splitting of the water droplet placed on it as a supply. The "cutting" of the supply droplet to dispense smaller droplets is largely dependent on the size of the transport electrode as well. Larger electrodes with a smaller electrode gap have shown to make dispensing easier [34]. The reservoir presented here is asymmetrical, and causes the supply droplet to "choose" the more advancing side of the reservoir, i.e. the side closer to the transport electrodes. This leads to inconsistent splitting and a tail formation, as seen (figure 3.11). The shape of the reservoir electrodes was also seen to affect the droplet necking position leading to the droplet cutting [35]. Indeed, the consistency location of the pinch-off is stated as a crucial factor in droplet splitting and relies on several parameters such as the volume of the reservoir drop, the surface properties and the applied voltage. It has also been speculated that the irregular droplet dispensing is due to uncontrolled internal pressure difference between the liquid in the

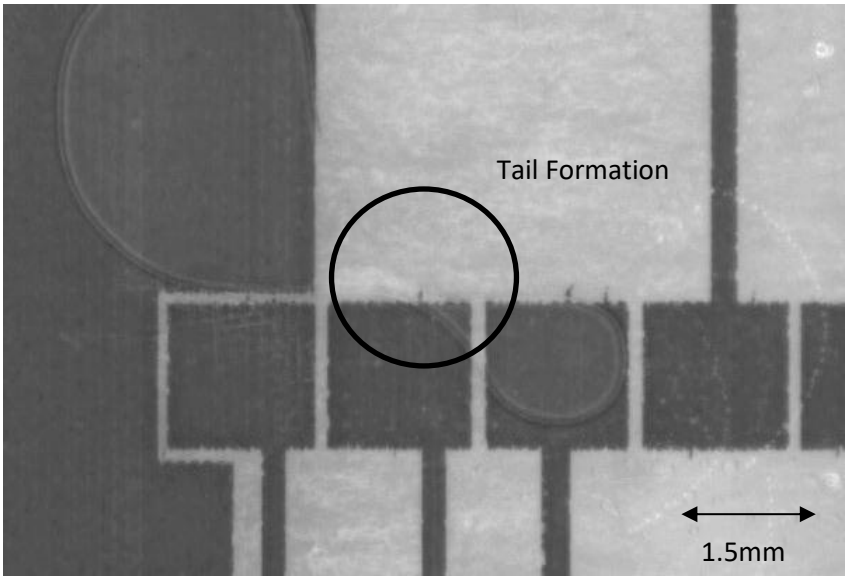

Figure 3.11: Tail formation after droplet splitting failure on a square electrode design

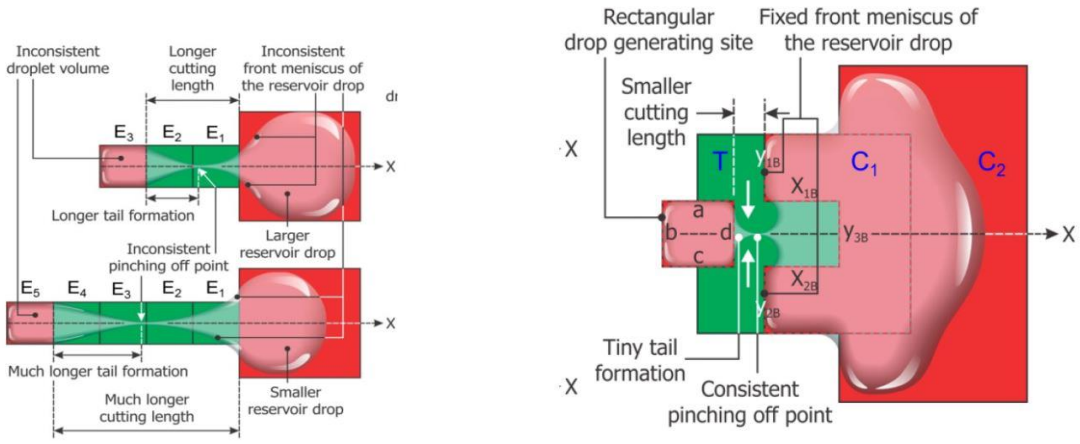

Figure 3.12 : Conventional splitting method in EWOD devices with related issues (left) and a potential solution for consistent splitting using a TCC reservoir (right) [35]

reservoir and the front of the liquid finger. This uncontrolled pressure difference varies the location of the front menisci of both the reservoir droplet and the dispensed droplet before cutting (figure 3.12).

Following this trail on droplet splitting, a new “TCC” reservoir electrode design was adopted [35]. It comprises four patterned electrodes, designed to help neck the droplet at the same location every time (figure 3.12). The designs were magnified as they were meant for inkjet-printed devices. The reservoir electrodes dimensions are, from far to center: 11mm x 6mm, 6.8mm x 4mm, 6.2mm x 3mm. The two variations of this pattern, one with a square center electrode (2mmx2mm) and one with a drop shaped electrode were drawn (figure 3.13).

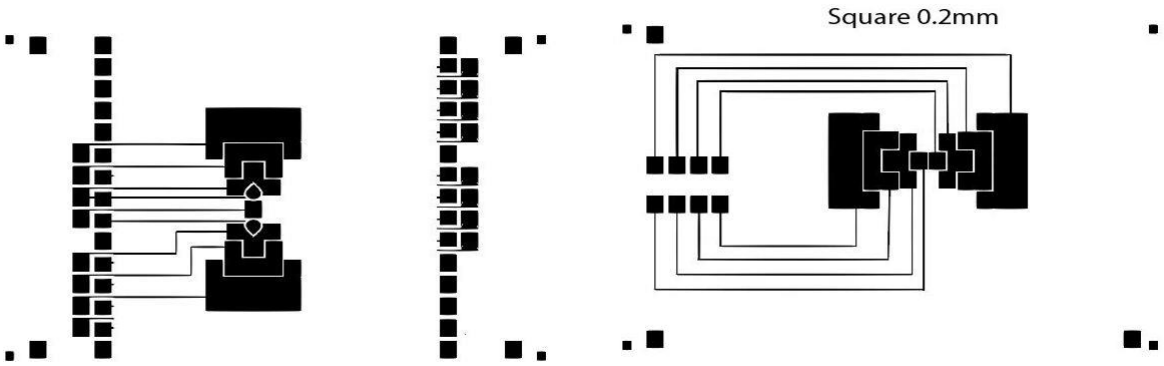

Figure 3.13: Design with TCC patterned electrodes for easier splitting adapted for IJP devices

Difficulties were encountered with the TCC design as well. These designs resulted in a significant number of shorted electrodes due to the unpredictability of the inkjet printer's output of ink (figure 3.14). The square shaped center electrode design was the most successful, as it presented the least shorts in the designs created.

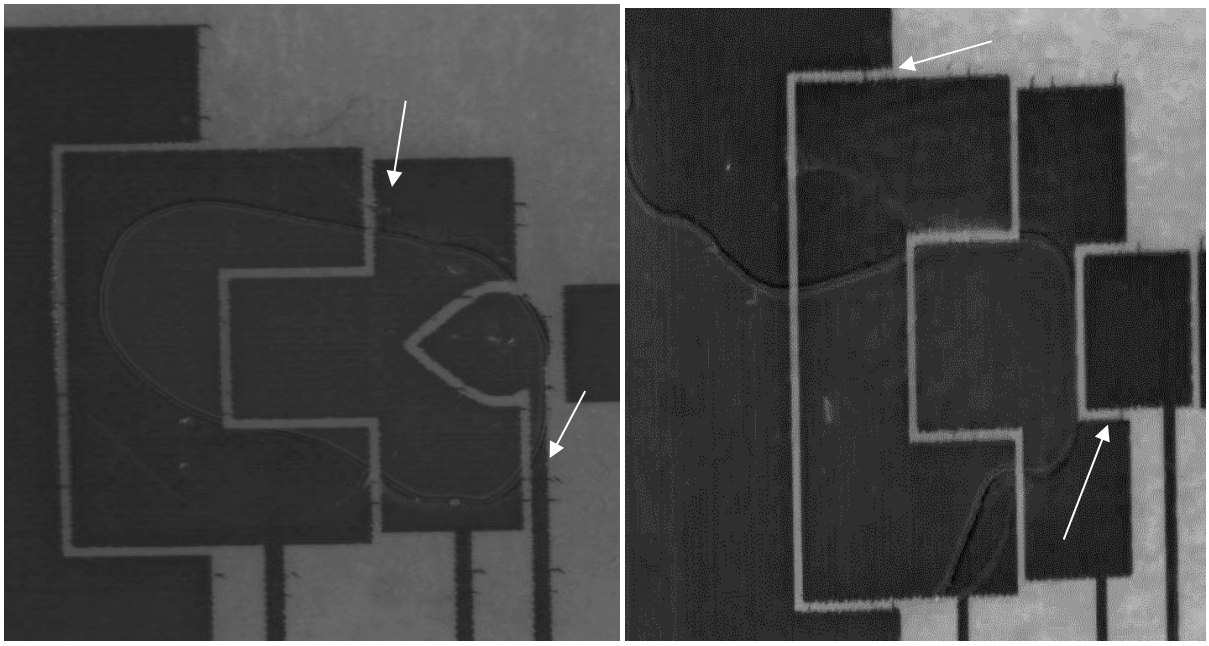

Figure 3.14: Pictures showing shorts between electrodes due to ink overlapping electrodes on the drop-shaped pattern (left) and the square pattern (right).

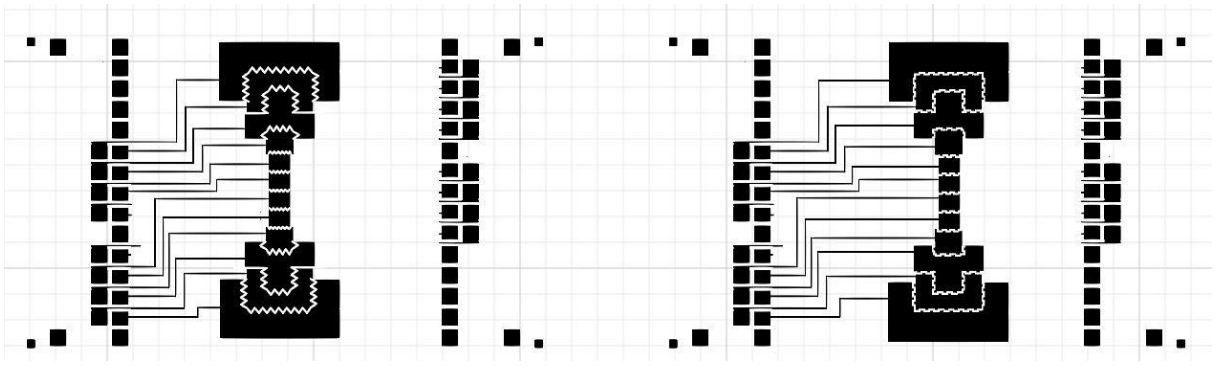

Figure 3.15: Design of interdigitated TCC electrodes in two variations: triangle (left) and square (right)

The next step in the design variation consisted of interdigitating the reservoir electrodes in order to help droplet splitting and facilitate droplet movement. Two patterns of interdigitation, square and triangle, were tried (figure 3.15). Electrodes were also drawn bigger in order to facilitate dispensing: 2mm by 2mm. A last design attempt consisted of adapting a design from Dixon et al, 2016 [30], presenting different shapes for the reservoir and dispensing electrodes (figure 3.16). The transport electrodes were star shaped. The elongated dispensing electrodes are drawn to help cut the droplet by elongating it from the reservoir onto the transport electrodes.

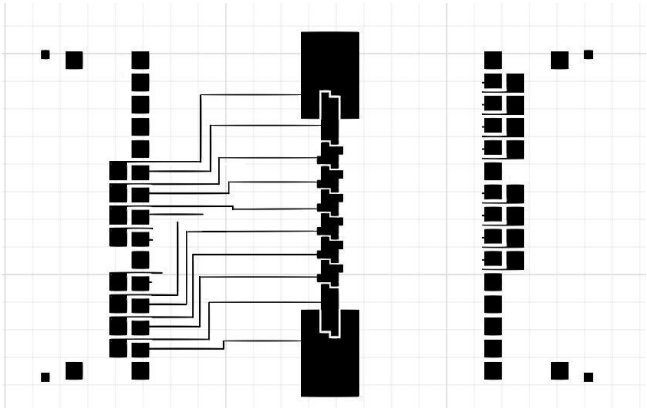

Figure 3.16: Design adapted from Dixon et al with a star transport electrode design for inkjet-printed devices [30]

Moving the droplets on the transport electrodes was successful on the interdigitated designs. Most of the star designs that were printed manifested too many shorts to be usable. This suggests that the design had probably not been adapted well to the IJP device design requirements. Dispensing the droplet from the reservoir wasn't successfully consistently executed. Various factors such as the inconsistencies in printing and spin coating presented obstacles (figure 3.17).

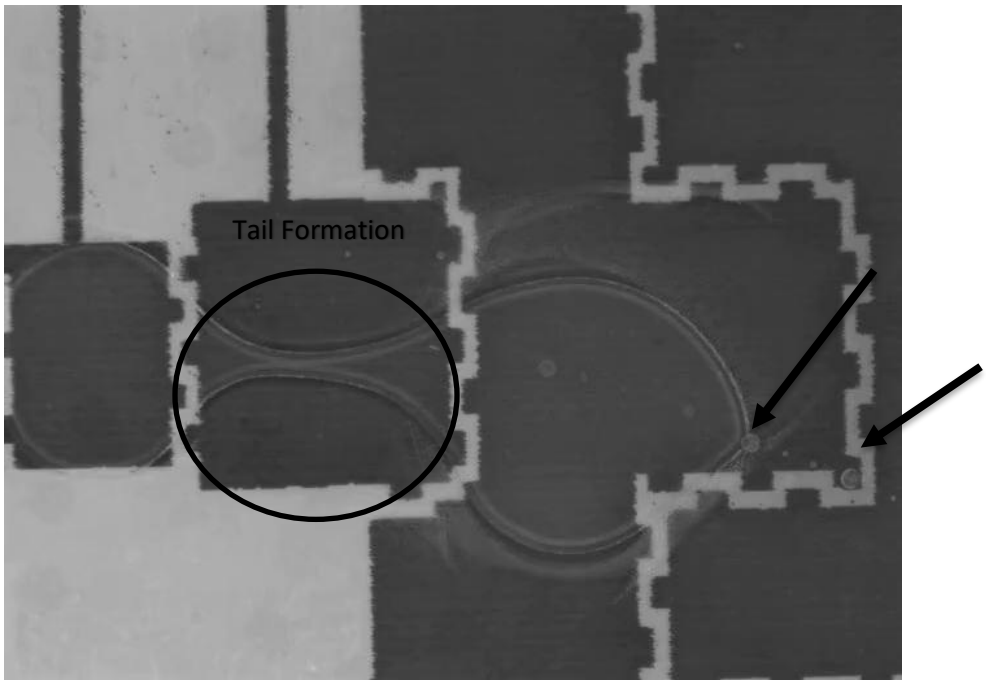

Figure 3.17: Splitting failure on the TCC interdigitated design (square). The beads shown by the arrows (spincoating inconsistencies) present on the surface of the device pin the droplet and inhibit its movement.

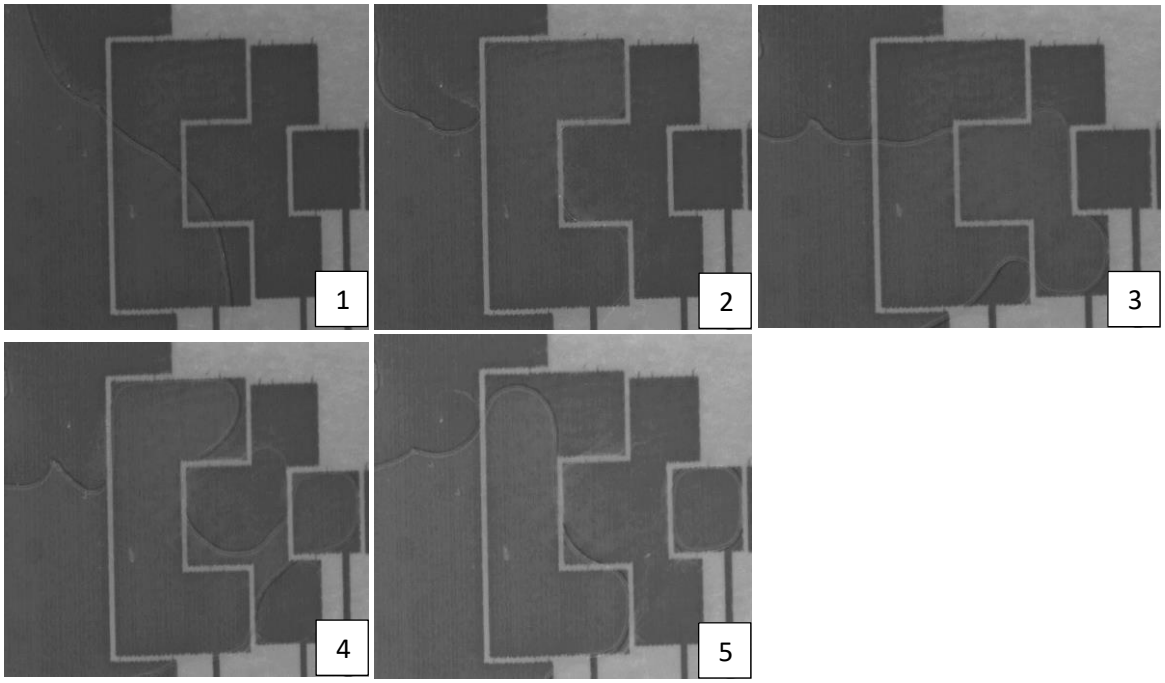

Figure 3.18: Dispensing a 4μL droplet from a TCC reservoir in a square shaped TCC designs with (1-3) elongation of the supply droplet in the reservoir then (4-5) cutting of the droplet

However, the TCC pattern design has shown promise for splitting (figure 3.18).

3.2 Device Operation

The equipment used in the experiments discussed remained unchanged throughout the course of the study (figure 3.19). The apparatus employed consisted of:

- A signal generator (NI PXI 5402)
- A digital multimeter (NI PXI 4072)

Both housed in NI PXI 1033 chassis

- A voltage amplifier (Trek PZD700A)
- IJP DMF device with pogo pin board controller

The voltage and frequency desired were set on the signal generator, which had a maximum input value of 5V peak-to-peak ($5V_{pk}$), then ramped up by a factor of 200 through the voltage amplifier and sent to the DMF device. The amplifier sends another signal that is stepped down by a factor of 200 to the digital multimeter which reads the voltage root-mean-squared value (V_{RMS}) coming out the amplifier, in order to make sure the voltage applied is correct. The images and videos were captured using a Zeiss stereo discovery V8 and a Zeiss axiocam for low-light and fluorescent applications (figure 3.20)

Figure 3.19: Signal generator with digital multimeter in chassis (left), voltage amplifier (middle), and pogo pin board from the Wheeler laboratory to control the DMF (right)

Figure 3.20: Zeiss stereodiscovery V8 microscope (left) and Zeiss axiocam MRm(right)

The objective of this study was to test whether DNA ligation can be executed on an inkjet-printed digital microfluidic device (figure 3.21).

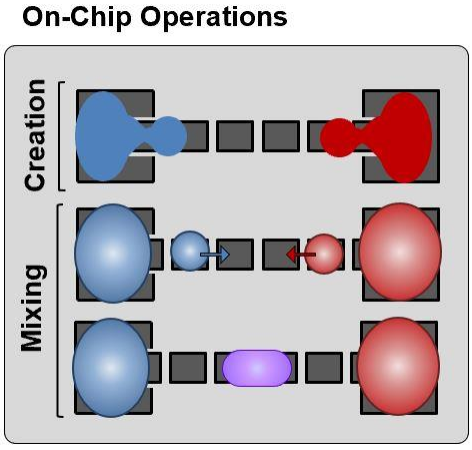

Figure 3.21: Operations to be performed on the IJP DMF for DNA ligation (courtesy of Dr. Schertzer)

The operations on the IJP device consisted of dispensing two droplets from two reservoirs containing two different bricks of DNA, then merging both daughter droplets to initiate the ligation, and finally mixing them by moving the merged droplet back and forth on the device. Each type of operations can be broken down into steps explaining how they get executed on the device. There are similarities when it comes to moving and merging on each device, as the designs don't much affect the moving sequence of the droplet much. The electrode contingent to the droplet is actuated in order to move the droplet. Dispensing changes depending on the design, as some designs have more reservoir electrodes dedicated to dispensing droplets. An example of electrode actuation can be found below (figure 3.22) for each design type: the square type design will have the same actuation sequence as any other design with one reservoir electrode such as the star design, and the TCC designs will have the same actuation sequence as its interdigitated variations. The electrodes were actuated manually by applying an AC voltage to the bond pad associated to them or by activating the Labview sequence corresponding to the wished operation: dispense/create and move/merge/mix (Appendix A). Applying voltage manually was crucial during the course of this study as the geometry of the devices kept changing and so did the applied voltages, as described in table 4.1. It permitted to try out different voltages and test the upper and lower limits of the devices fabricated. Preliminary feasibility tests using deionized water droplets has been done in order to verify that the designs used can perform the operations successfully and repeatably, and the voltages applied are within operational range of the device.

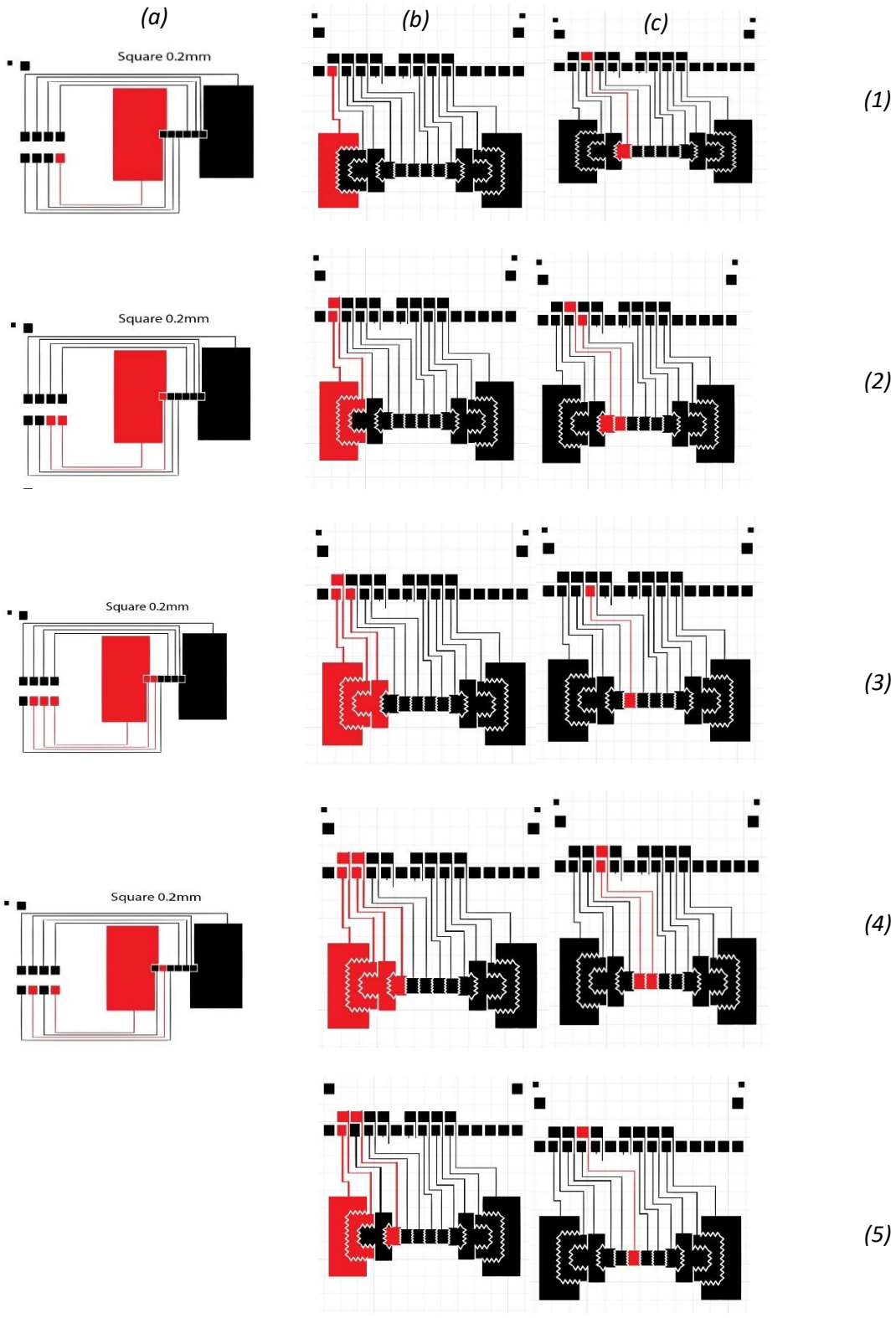

Figure 3.22: Actuation sequence (1-5) for droplet dispensing on a square design IJP (a) and on a variation of TCC design (b), and a general actuation sequence for moving droplets on the transport electrodes from left to right (c)

3.3 Ligation and Gel Electrophoresis

This part of the experiment can be broken down into simple steps for three different scenarios:

1. Ligation

    i. Bench experiment (Eppendorf Tube):

        (a) Droplet containing DNA brick 1

        (b) Droplet containing DNA brick 2

        (c) Ligation in Eppendorf tube

    ii. Merging on DMF device experiment:

        (a) Droplet containing DNA brick 1

        (b) Droplet containing DNA brick 2

        (c) Merge both droplets – ligation on DMF

        (d) Extract merged droplet for incubation in Eppendorf

    iii. Merging and mixing on DMF device experiment:

        (a) Droplet containing DNA brick 1

        (b) Droplet containing DNA brick 2

        (c) Merge both droplets

        (d) Move merged droplet back and forth to mix

        } ligation on DMF

        (e) Extract merged and mixed droplet for incubation in Eppendorf

2. Two step incubation in Eppendorf tube:

    i. 30 minutes at 37C

    ii. 10 minutes at 70C

3. Gel electrophoresis:

    i. Place harvested droplets after incubation in gel and run gel electrophoresis

    ii. Examine results using fluorescent scanner

The bench top ligation protocol was provided by the industrial partner. It was tested on the bench first for confirmation of successful ligation, before altering the protocol to adapt it to the digital microfluidic device's operations. The initial mixing volume was of a total of 20μL and contained:

Table 3.1: Reagents present in initial mixture for bench top DNA ligation

Reagent	Volume (μL)
DI Water	10.5
T4 DNA ligase buffer (10X)	1.2
Brick 1 (5μM)	4.0
Brick 2 (5μM)	4.1
T4 DNA ligase	0.2

This was modified with the help of Dr. Michel from the College of Science to perform a simpler yet successful ligation on the bench, while keeping some of the proportions of the mixture. The following mixture was used for bench procedure in an Eppendorf tube:

Tube 1: 1µL of Brick 1 + 4µL of DI Water – (5µL)

Tube 2: 1µL of Brick 2 + 4µL of DI Water – (5µL)

Brick to total volume ratio 1:4

Following the bench ligation, the mixture was incubated at room temperature for one hour. Proteinase K and calcium chloride were added to the mixture, and incubated for 30 minutes at 37C in an air incubator then 10 minutes at 70C in a water bath. This step insured the elimination of any bound T4 DNA Ligase, which would cause aberrant DNA electrophoretic migration.

The DMF procedure required the inclusion of a surfactant to limit biofouling and help the droplets move easier as proteins and other biological material tend to stick to the surface of the device. Tween 20 at 0.1% concentration per volume was employed as a surfactant, using the following proportions:

Tube 1: 5µL of Brick 1 + 2.5µL Tween 20 (1%) + 17.5µL DI Water – (Total volume = 25µL)

Tube 2: 5µL of Brick 2 + 2.5µL Tween 20 (1%) + 17.5µL DI Water – (Total volume = 25µL)

The droplets manipulated on the device were taken from those prepared solutions and harvested off once the mixing procedure and incubation at room temperature on the device were done. The two-step incubation (37C and 70C) on the DMF device directly has been attempted, but a decrease in droplet areas due to evaporation over the course of this incubation discouraged this procedure (figure 3.23). A wet sponge was used under the device to try and decrease the evaporation rate of the droplets by increasing the humidity of its environment.

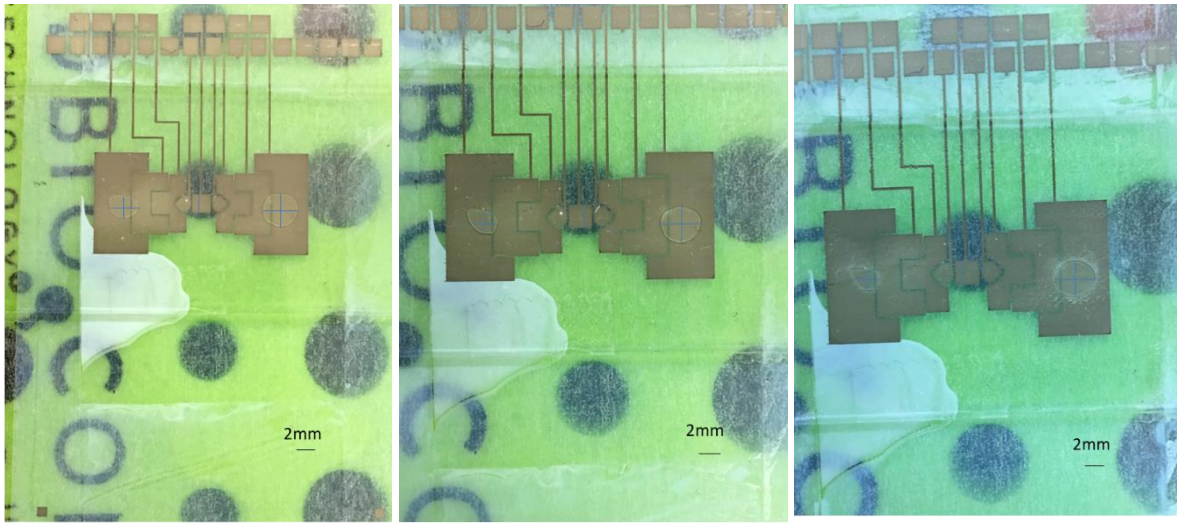

Figure 3.23: Droplet area differences for 1µL droplet and 2µL droplet before incubation (left), after incubation at 37C (middle), and after incubation at 70C (right).

After the incubation, the DNA gel electrophoretic migration could be examined. In order to execute this process, an agarose gel at 2% was prepared and 2µL of ethidium bromide was added. It was then loaded into the electrophoresis rig and allowed to cool for 30 minutes.

Four solutions are prepared for the gel run:

1) 9µL DI water + 2 µL Dye (Purple) + 1µL Brick 1 (prepared) - (Total Volume=13µL)
2) 9µL DI water + 2 µL Dye (Purple) + 1µL Brick 2 (prepared) - (Total Volume=13µL)
3) 9µL DI water + 2 µL Dye (Purple) + 1µL Ligated (on/off device) - (Total Volume=13µL)
4) Ladder Solution: 1 µL Ladder + 1 µL Dye + 4 µL DI Water – (Total Volume=6µL)

The gel was run at 95V for 50 minutes (figure 3.24), and was analyzed in a fluorescent scanner set for ethidium bromide. The electrophoretic migration of the DNA bricks from the negative to the positive in the solutions prepared for the gel run inform us of whether the ligation was successful. The bench experiment performed initially served as a reference for future ligations. A process flow chart for the ligation protocol can be found in figure 3.25.

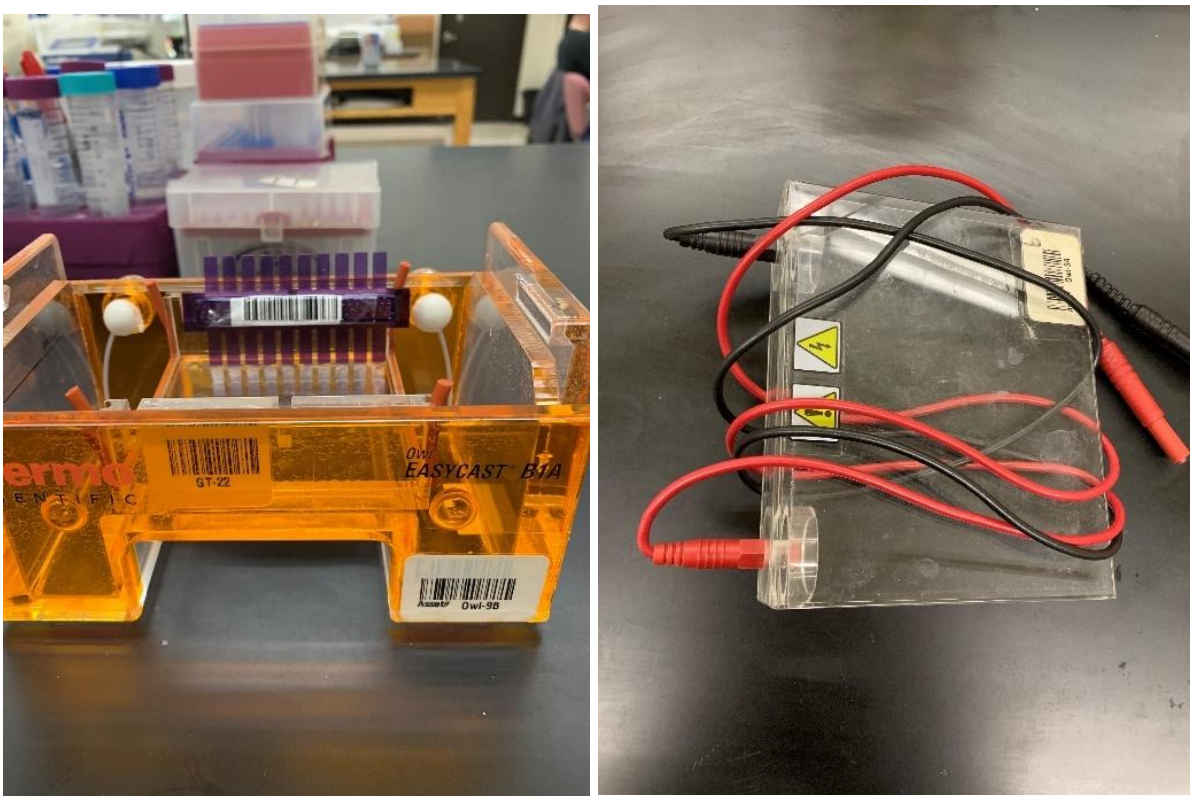

Figure 3.24: Gel electrophoresis rig + gel comb (left) and the cover with the anode and cathode (right)

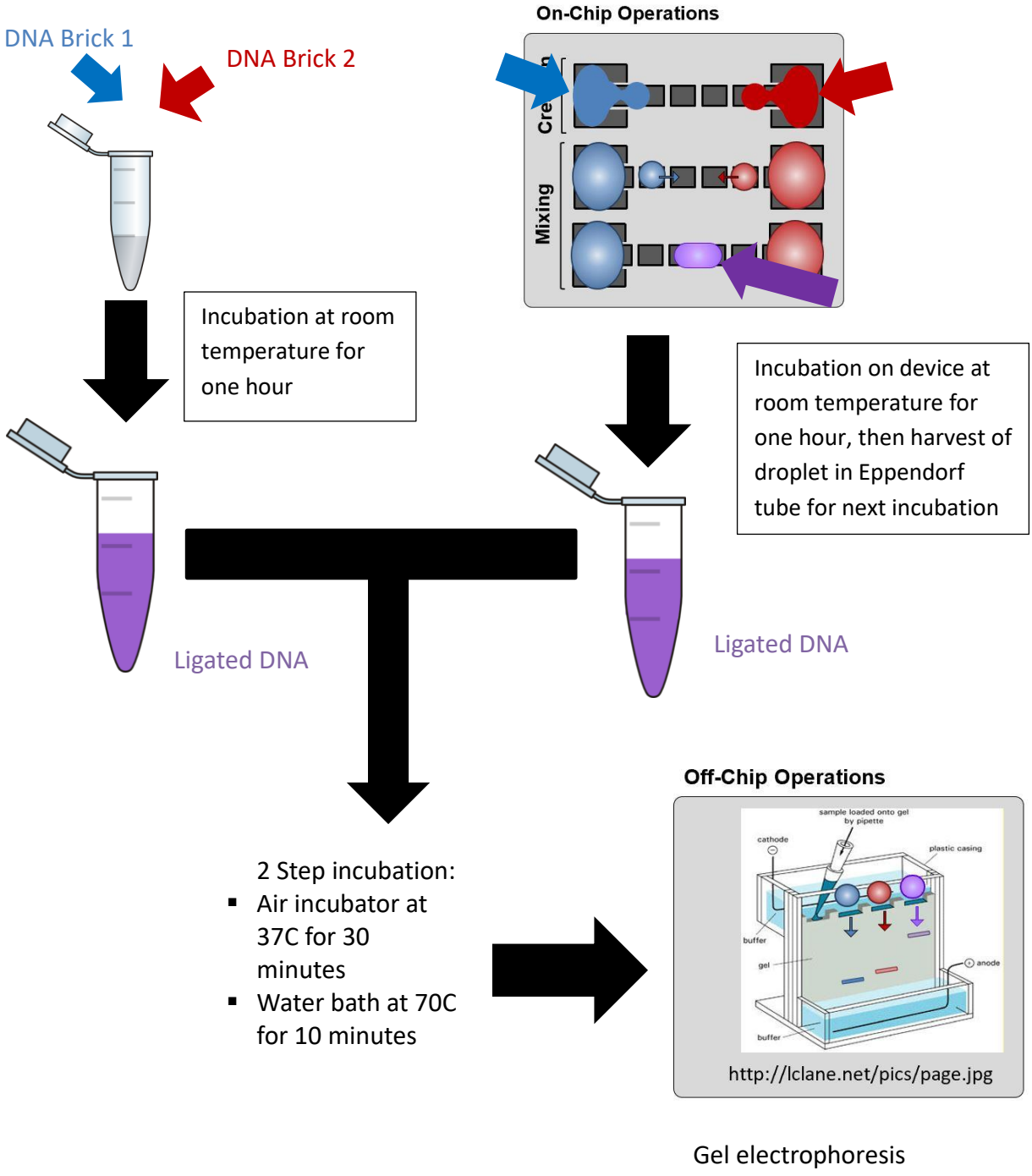

Figure 3.25: Process for DNA ligation on bench and on device, followed by incubation and gel electrophoresis

4.0 RESULTS AND DISCUSSION

This section will discuss results obtained during this study. The effects that certain parameters, such as the design of the device and the droplet size, have on the device operations are investigated. We will examine the effect of the design on the voltages applied on the devices, and note the droplet volume used for the operations on each of those devices.

4.1 Preliminary testing with DI water droplets

The evolution of designs throughout this study sought to improve device operations. As such, the manufacturing yields relating to each design represented in Table 4.1 help understand which designs are "favorable" for IJP devices.

Table 4.1: Production yield of devices by design

	Printed	Coated	Usable	Final Yield (%)
Square	36	22	14	38.9
TCC Square	12	7	4	33.3
TCC Droplet	12	7	3	25
TCC Inter Square	24	14	11	45.8
TCC Inter Triangle	16	7	3	18.8
Star	16	0	0	0

The above table shows the devices with the most yield were the initial square designs and the TCC interdigitated square designs, with respective yields of 38.9% and 45.8%. Once the designs were printed, they were tested for shorts between electrodes by checking for continuity with a multimeter. Factors such as device geometry, design complexity and printing orientation were among the main reasons for a variation in reliability and consistency in printing. Indeed, the TCC droplet, the TCC interdigitated triangle and the star designs had the least yield as the droplet shape, the interdigitated spikes, and the star were not "printer friendly" designs, showing

too many shorts. Most of the TCC designs manifested too many shorts due to the complexity of the design. The square design printing improved by switching the design orientation to vertical to "help" the printer and minimize the overlapping of ink between electrodes. Those deemed to have too many shorts to perform the device operations (dispense, split and/or move, merge, mix) were not coated. Additionally, many devices were unusable after the spin coating stage due to the presence of solid beads on the surface of the device, as shown in figure 3.17. These beads pin droplets and make moving them more difficult. The cause of this phenomenon has not been discovered during this study.

Table 4.2: Test matrix for voltage ranges and operation success on each device type

Design	Operation Performed	Frequency Applied (kHz)	AC Voltage Applied (V_{RMS})		Success?
			Min	Max	
Square	Dispense/Split	1	73.4	96.1	Yes*
		10	73.4	96.1	Yes*
		100	91.2	120	Yes*
	Move/Merge/Mix	1	65	95.3	Yes
		10	65	95.3	Yes
		100	82.6	112	Yes
TCC Square	Dispense/Split	1	52.1	74.3	Yes*
		10	52.1	74.3	Yes*
	Move/Merge/Mix	1	46.4	74.3	Yes
		10	47.8	77.8	Yes
TCC Droplet	Dispense/Split	1	51.3	71.2	No
		10	51.3	73	No
	Move/Merge/Mix	1	46.4	75.9	Yes*
		10	43	76	Yes*
TCC interdigitated square	Dispense/Split	1	57.8	71	No
		10	60.5	73.2	No
	Move/Merge/Mix	1	54.2	60	Yes
		10	61.3	85.3	Yes
TCC interdigitated triangle	Dispense/Split	1	71.2	82.2	No
		10	76.9	85	No
	Move/Merge/Mix	1	68.4	72.7	Yes
		10	71	81.8	Yes
"Wheeler" Star	Dispense/Split	1	NA	NA	No
		10	NA	NA	No
	Move/Merge/Mix	1	NA	NA	No
		10	NA	NA	No

(**conditional success, not consistently repeated)*

Above are the results for testing the voltage ranges for each device, with the observation of whether operations can be executed repeatedly. In order to test the capabilities and limits of the printed devices, the range of voltages that could be applied for each design was examined in Table 4.2. These voltages range from the lower limit voltage where droplet movement was detected to the upper limit where electrolysis was encountered. Device operations are tested within those ranges and "ideal" droplet volumes for each type of operation have been noted on each device after repeated trials of different volumes. These preliminary tests were executed using DI water droplets to gauge the minimum volume needed to perform operations with droplets containing the DNA material for ligation.

During those tests, the volume of the droplet needed to execute the operations was noted in the table below:

Table 4.3: Droplet volumes chosen for each operation after repeated trial of the operation

Device	Operation	Droplet Size (µL)
Square	Dispense	4.5
	Move	2
TCC Square	Dispense	4
	Move	1.5
TCC droplet	Dispense	4
	Move	1.5
TCC inter square	Dispense	4
	Move	2
TCC inter triangle	Dispense	4
	Move	2
"Wheeler" Star	Dispense	NA
	Move	NA

As seen in the tables above, the star design adapted from Dixon et al [30] was not viable to perform any of the operations. Sources of error may include the adapted design dimensions not being suitable for the inkjet-printing resolution, as many electrodes were shorted after printing. Dispensing/splitting a droplet from the reservoir has not been successfully and consistently

executed repeatedly. Moving/merging/mixing was successfully repeated on the interdigitated variations of the TCC design. These devices were used to perform the ligation by merging (figure 4.1) and mixing (figure 4.2) the droplets containing biological material. The droplets were pipetted on the transport electrodes for manipulation on the device.

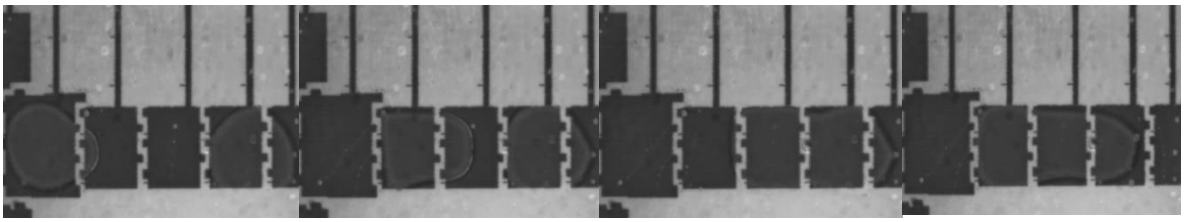

Figure 4.1: Merging of two droplets containing DNA material for ligation on a TCC interdigitated square device (from left to right)

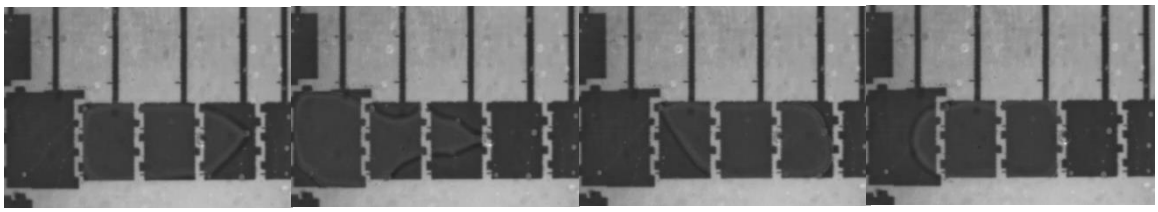

Figure 4.2: Mixing of the merged droplet containing DNA material for ligation on a TCC interdigitated square device (left to right)

4.2 Gel electrophoresis

The first bench DNA ligation gave us a reference on which number of base pairs each DNA brick should fall under approximately. After analyzing the electrophoretic migration (figure 31), it has been concluded that Brick 1 and Brick 2 fall around 150 base pairs, while the ligated brick falls under approximately 285 base pairs (between the 250 and 300 base pair mark):

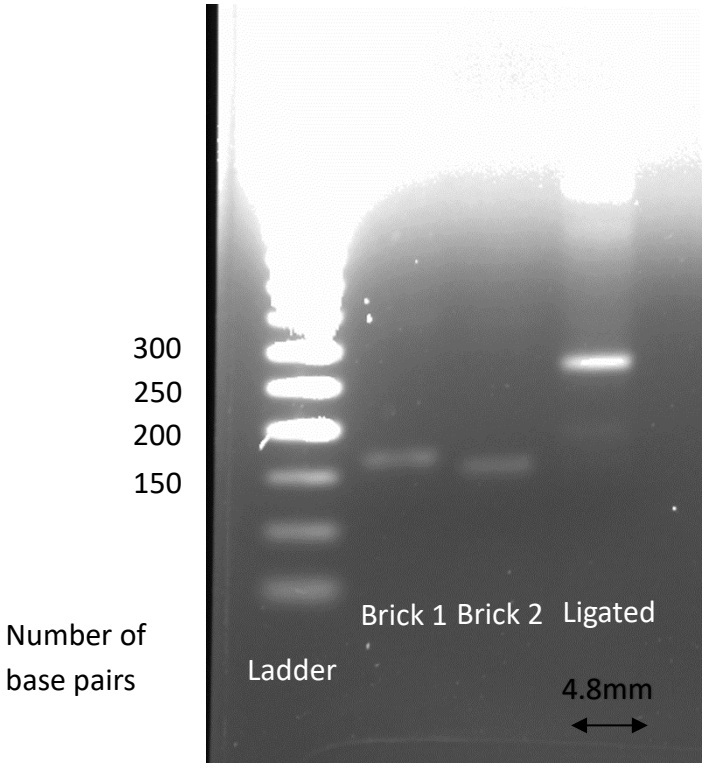

Figure 4.3: Gel electrophoresis result of first bench DNA ligation

The second experiment conducted merged both daughter droplets containing DNA brick 1 and DNA brick 2 respectively on the DMF device. Since dispensing was not successful, 2µL droplets were pipetted onto the device on the transport electrodes. The merged droplet was incubated on the device first for one hour, then harvested for the next incubation steps and gel electrophoresis with analysis. The result below suggests that the experiment was a success since the same number of base pairs was identified for the merged droplet on the DMF device and the ligated DNA on bench (figure 4.4).

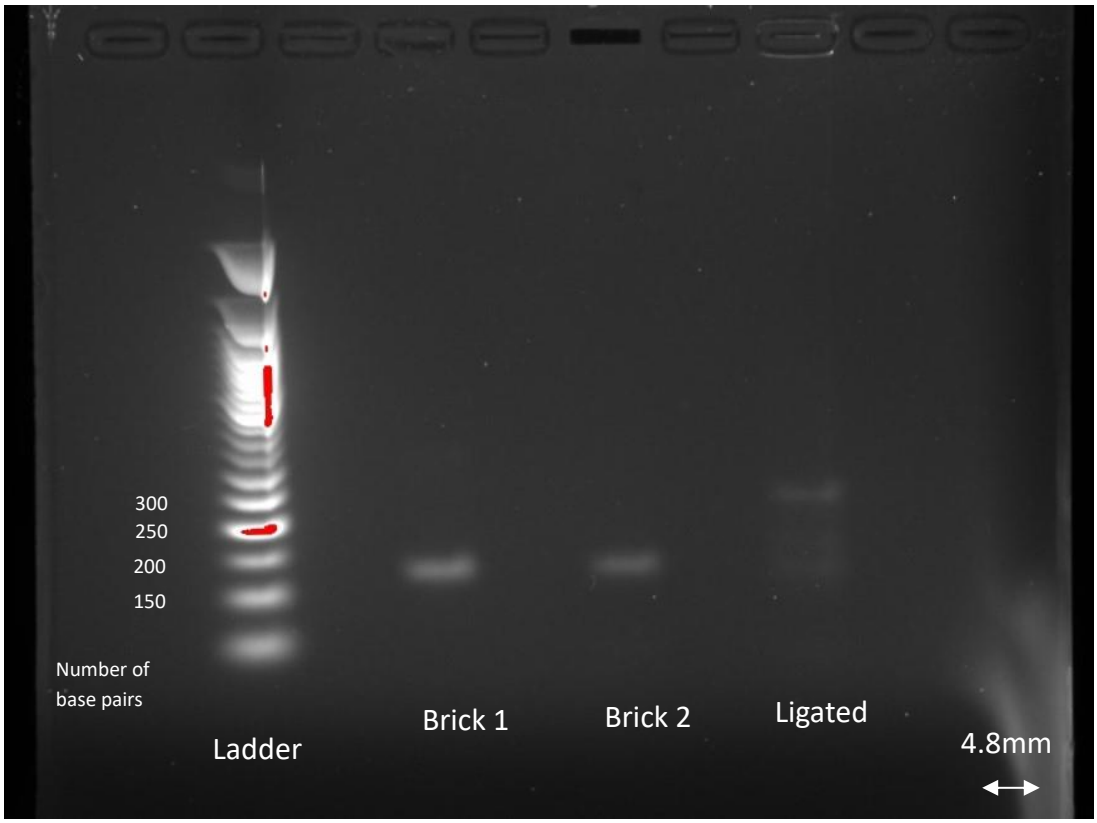

Figure 4.4: Electrophoretic analysis showing the weight of the DNA brick in the merged droplet to be the same as the ligated bricks on bench

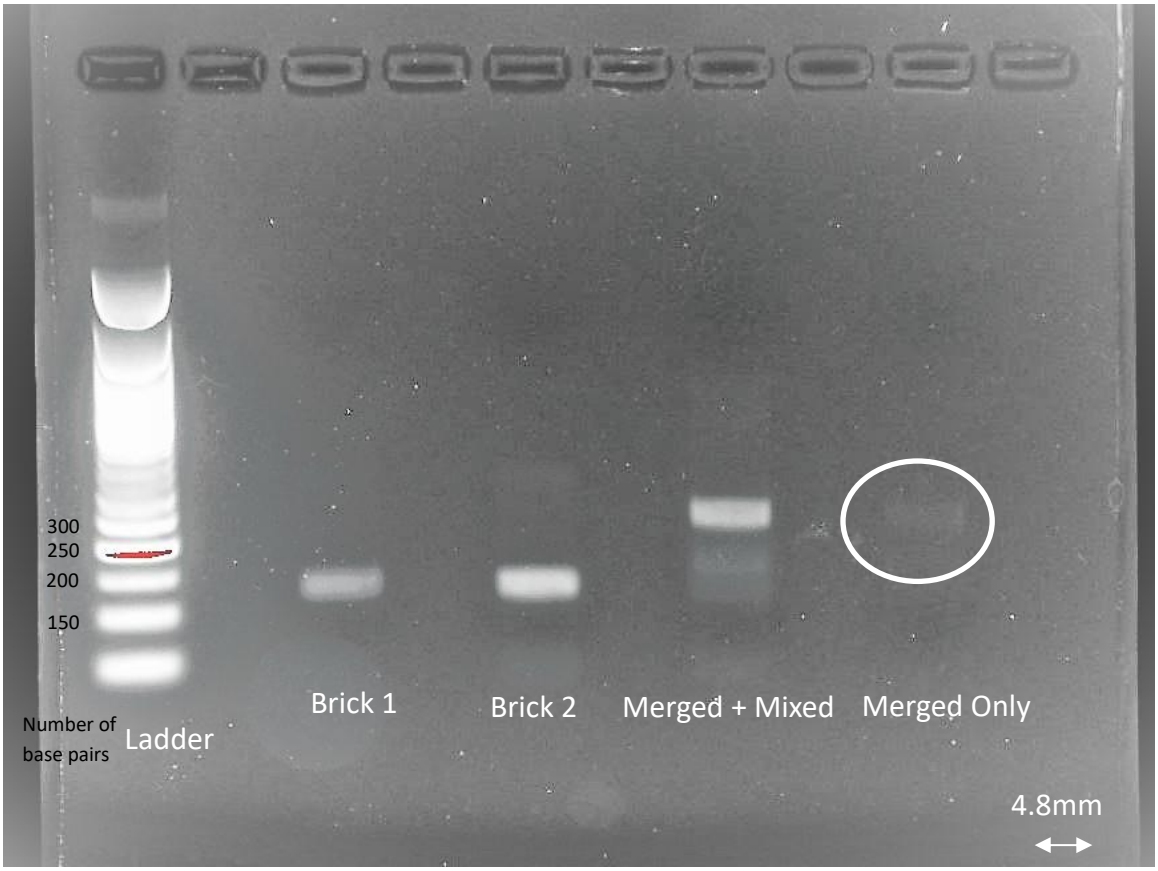

Figure 4.5: DNA Gel electrophoresis of a merged and mixed droplet on DMF device next to a merged only on DMF device

The same experiment was repeated, this time mixing the merged droplet by moving it back and forth on the device for a couple of minutes. The results confirm yet again that the ligation is possible on the DMF device (figure 4.5).

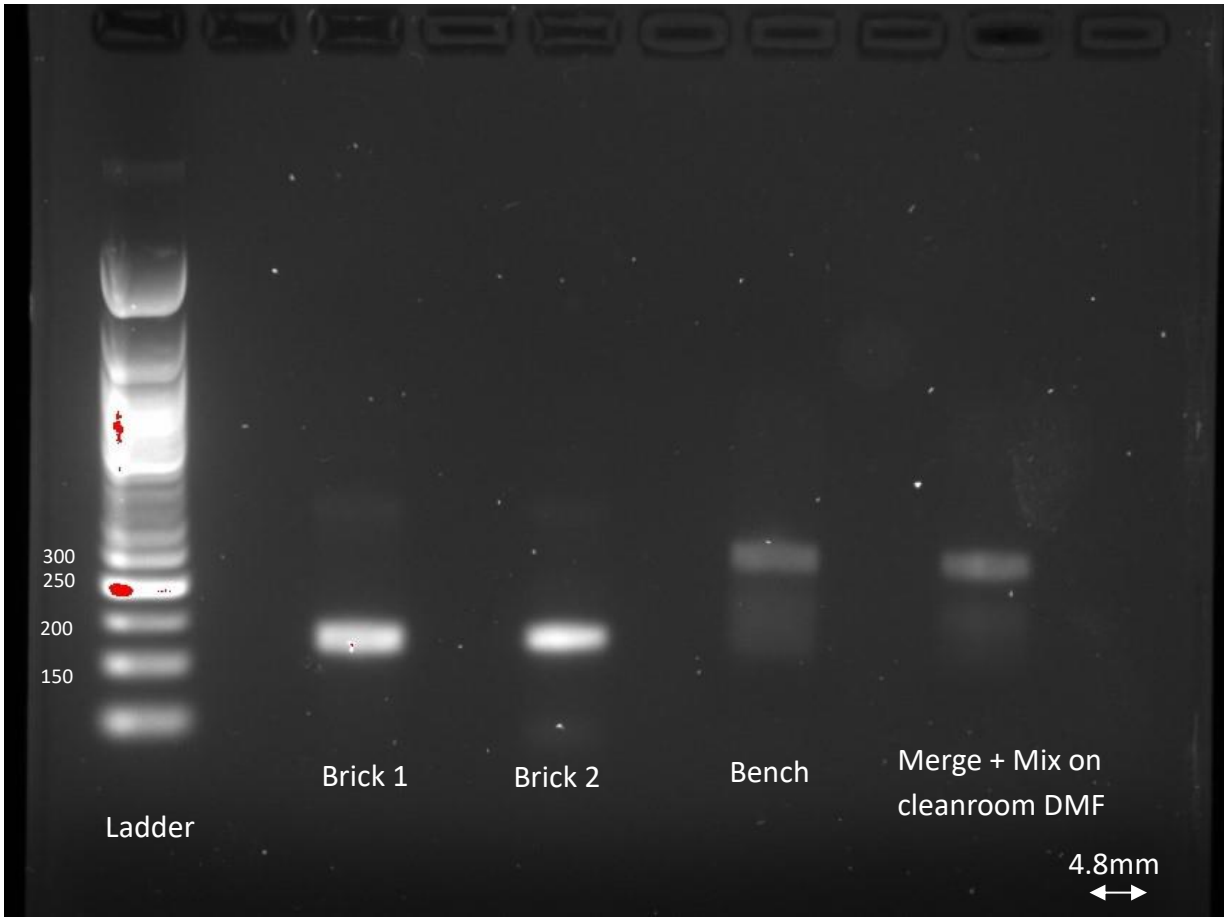

Figure 4.6: DNA gel electrophoresis results for a bench ligation vs a ligation of a merged and mixed droplet on a cleanroom DMF device

In parallel, the same successful experiment was also performed on a cleanroom fabricated DMF device by Hee Tae An (figure 4.6). This suggests that IJP DMF devices may be able to perform the same operations as the cleanroom fabricated DMF devices for a fraction of the cost of manufacturing and be employed for some experiments that don't require a complex device structure.

5.0 CONCLUSIONS

5.1 Summary

This study sought to investigate whether DNA ligation was possible on an inkjet-printed digital microfluidic device, as a first step towards testing for oligonucleotide synthesis on a DMF device.

The industrial partner Nuclera Nucleics created a DNA ligation protocol using water as medium, rather than the traditional organic solvent acetonitrile. This opens the door to a potential application in microfluidics, particularly in digital microfluidics, where droplets are individually controlled to perform various operation such as splitting, merging, dispensing and moving. Digital microfluidics is attractive as it requires less reagent and it can execute various tasks in a short amount of time. This study specifically examined if this protocol could be adapted and performed on inkjet-printed digital microfluidic devices, a low-cost alternative for cleanroom fabricated digital microfluidic devices. These low-cost devices are manufactured in a shorter amount of time and for a fraction of the cost compared to the traditional cleanroom devices. The goal was to check whether the operations performed on a cleanroom fabricated DMF device can also be performed on a low-cost IJP DMF device. Thus, a total of six designs were tested with DI water droplets in order to make sure that basic operations such as moving and dispensing droplets could be performed.

As stated in section 4.1, the dispensing/splitting of droplets on the IJP devices was not successful on any device. However, moving/merging/mixing was successfully repeated consistently on most devices, and the interdigitated variation of the TCC design was chosen to

perform operations with droplets containing biological material for DNA ligation. As a result, the droplets were pipetted on the transport electrodes for easier manipulation.

In order to verify whether the ligation on the DMF device was successful, it was necessary to perform a bench top ligation using the protocol provided. A gel electrophoresis was then executed to establish a reference for the migration of the DNA bricks individually and ligated (figure 4.3). Two scenarios were then put in place for the experiment on DMF device: one where the droplets containing DNA material are merged only, and one where they are merged and mixed by moving the merged droplet back and forth on the device. The gel electrophoresis comparison confirmed that the ligation is successful on the IJP DMF device for both scenarios, as the electrophoresis migration of the ligated bricks was the same (figures 4.3, 4.4., 4.5). Finally, the ligation tested in parallel on a cleanroom DMF device also presented the same results (figure 4.6), suggesting that some operations can similarly be performed on the IJP device without adversely affecting the outcome.

5.2 Contributions

The success of DNA ligation on a DMF device is just a stepping stone to the ultimate goal of this research: performing oligonucleotide synthesis on a DMF device. Those DNA chains currently have to be manually assembled by scientists and can be expensive and time-consuming. Having easier access to fabricating long chains of DNA can further the advancements in biomedical fields such as epigenetics and drug development. Adapting DNA synthesis on these devices can alleviate the bottleneck created by the lack of supply vendors for long chains of DNA (more than 3000 base pairs). Indeed, combining the aqueous chemistry created by Nuclera Nucleics with the automatability of the DMF device could be a potential candidate for a “lab on

a chip" device. The success of the DNA ligation on a DMF device shows that the chemical innovation brought by the industrial partner is compatible with the fluid handling capabilities of this type of device.

5.3 Future Work

The DNA ligation executed is but the first step in a larger scope. The end goal of this research is to be able to synthesize oligonucleotide chains on the surface of the device directly, by exploiting the novel aqueous chemistry combined with the DMF device operations. It is possible that the next DNA synthesis procedures require magnetic beads as bases for building longer chains, which will then require to be separated and washed between steps to get rid of any excess reagent. The latter will occur by immobilizing the beads on the surface of the device using a magnet, and by manipulating the washing buffer to pass over the beads. Preliminary research regarding oligonucleotide synthesis and separation procedures on DMF devices has been done in order to prepare for the future endeavors.

While oligonucleotide synthesis has not been performed in DMF devices, a similar process of particle separation and washing has been performed in DMF immunoassays [22, 23]. Immunoassays use antibody-antigen interactions to bind biological material to a solid surface in order to test for the presence and concentration of target proteins. This is useful for droplet libraries and compound screens which provide tools for the function analysis of genomes, individual proteins or complexes [36]. It is also useful for directed evolution of enzymes [37], or DNA analysis and PCR (Polymerase Chain Reaction) [38]. However, immunoassays require a large volume [29], a big cost and amount of time for each assay [5]. While Solid Phase

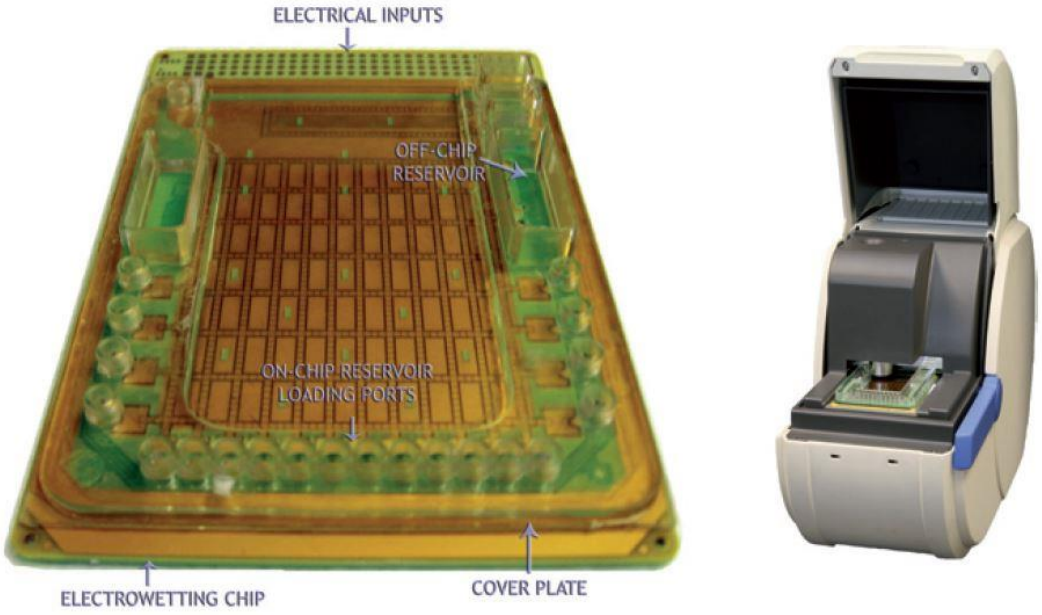

Figure 5.1: DMF immunoassay and its control system [5]

Oligonucleotide Synthesis has not yet been carried out on DMF devices, it is useful to examine how unbound reagents are frequently separated and/or washed away on the immunoassay device.

Magnetic filtration relies on the magnetic force of a magnet to hold the magnetic particles in place while the separation takes place. In droplet-based magnetic immunoassays for instance, a droplet of the sample and a droplet of the reagent containing the magnetic beads are merged and incubated. After the formation of antibody-antigen complex, the magnetic beads are immobilized and any unbound material is washed away (figure 5.2). A reagent droplet for detection is added to quantitively evaluate the washing and retention efficiencies [28]. The choice of magnet employed and its location are crucial design parameters in magnetic filtration on DMF. A neodymium N48 grade with a 15.3lb pull force, 5/8 inches diameter and ¼ inch thickness may be used [29]. Other neodymium N42 magnets with different pull forces (1.25lb, 5lb, 10lb) were also employed. They were positioned over and/or under the device when beads

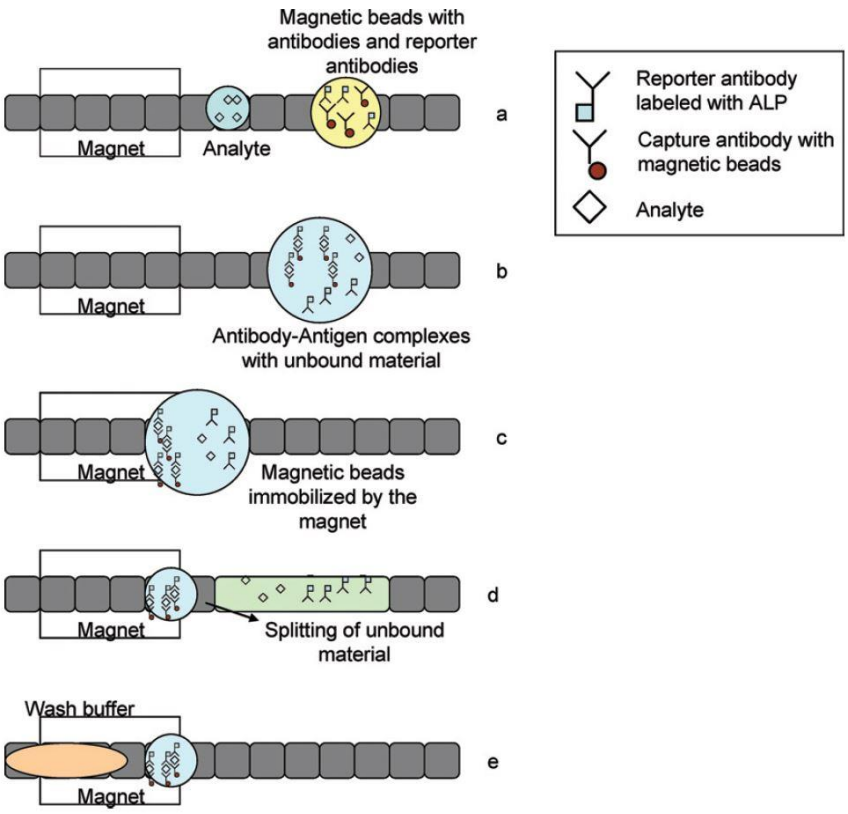

Figure 5.2: Example of magnetic filtration with use of antibody-antigen complexes [28]

needed to be held still, and removed to allow beads to resettle in the droplet [28]. The future work is directed towards magnetic separation because it simplifies the microfabrication process by eliminating either the physical barrier on the surface required for mechanical filtrations [39], or the knowledge of "trap" locations in a confined geometry [25].

The separation and washing protocols are essential to ensure that the filtration has a maximum yield. Two methods are reviewed for future research: serial dilution and supernatant washing. In serial dilution washing, the DMF is used to merge and mix droplets of wash suspension with a droplet of wash buffer. The magnet is positioned in such a way that particles are immobilized to one side of the pooled droplet, and the droplet is then split into two daughter droplets. The droplet not containing particles is put to waste. The bead droplet is then washed with a surfactant

to prevent bead aggregation. The process is then repeated as needed (four [29] or five [28] times) (figure 5.3). In supernatant separation washing, the particles are also mixed with wash suspension solution, then immobilized by the magnet. The DMF is used to actuate the supernatant droplet away from the magnet to waste, leaving particles on the device surface. Once the magnet is removed, a droplet of wash buffer is added to resuspend the particles. The supernatant is transported away and collected after every wash. Like serial dilution, the process is then repeated as needed (figure 5.4).

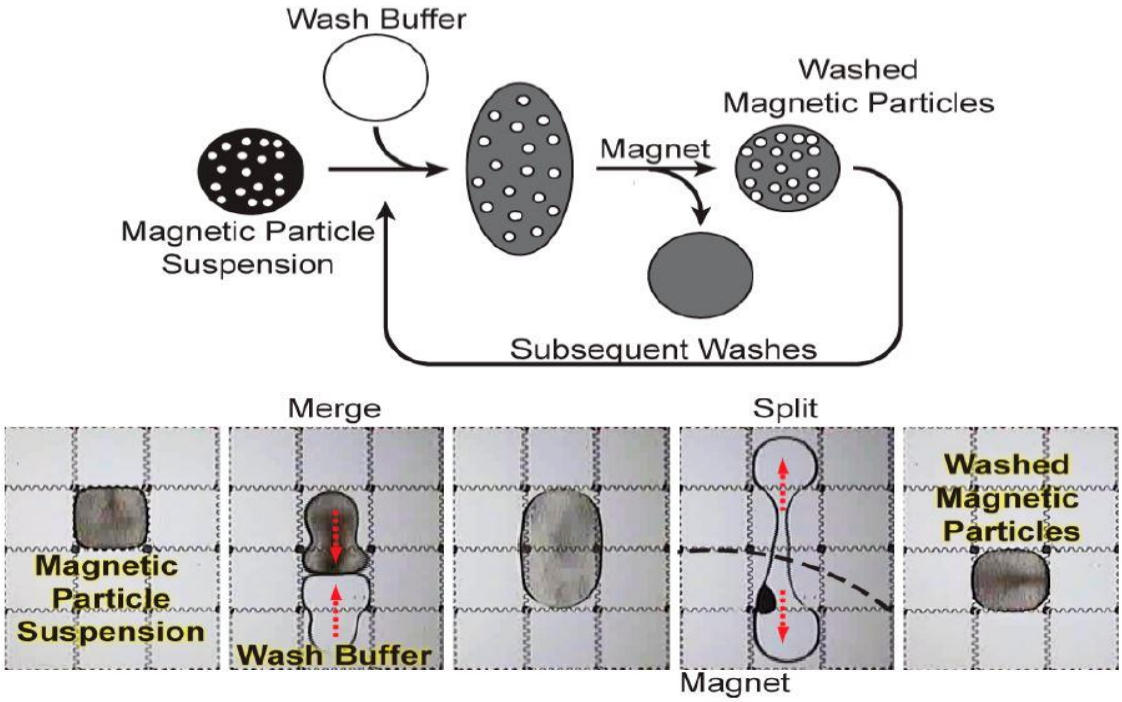

Figure 5.3: Serial Dilution washing process [29]

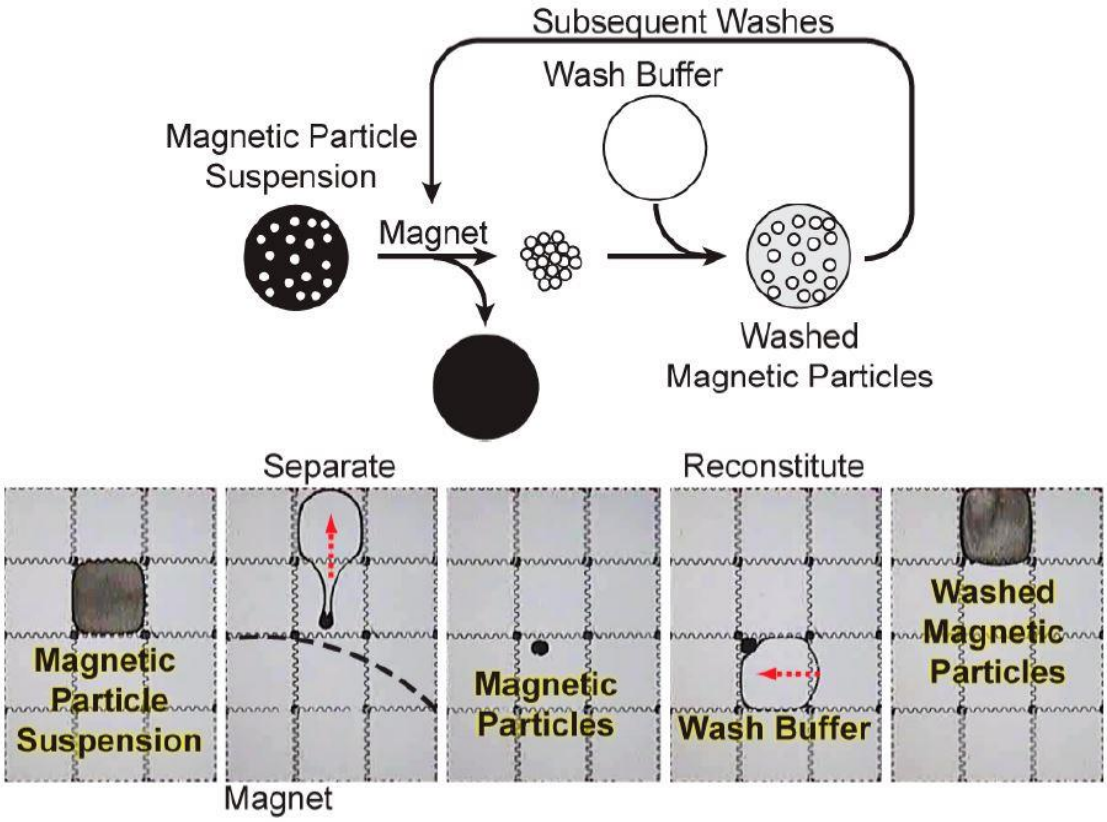

Figure 5.4: Supernatant separation washing protocol [29]

Washing efficiency is higher for supernatant washing than serial dilution. This means that less washes are required to attain a desired threshold of reduction of unbound reactant when using supernatant washing (figure 5.5). This washing protocol will likely be adopted as one of the future aims of this research will surely include achieving the highest washing efficiency possible on a DMF device for droplets containing DNA on magnetic beads with magnetic filtration.

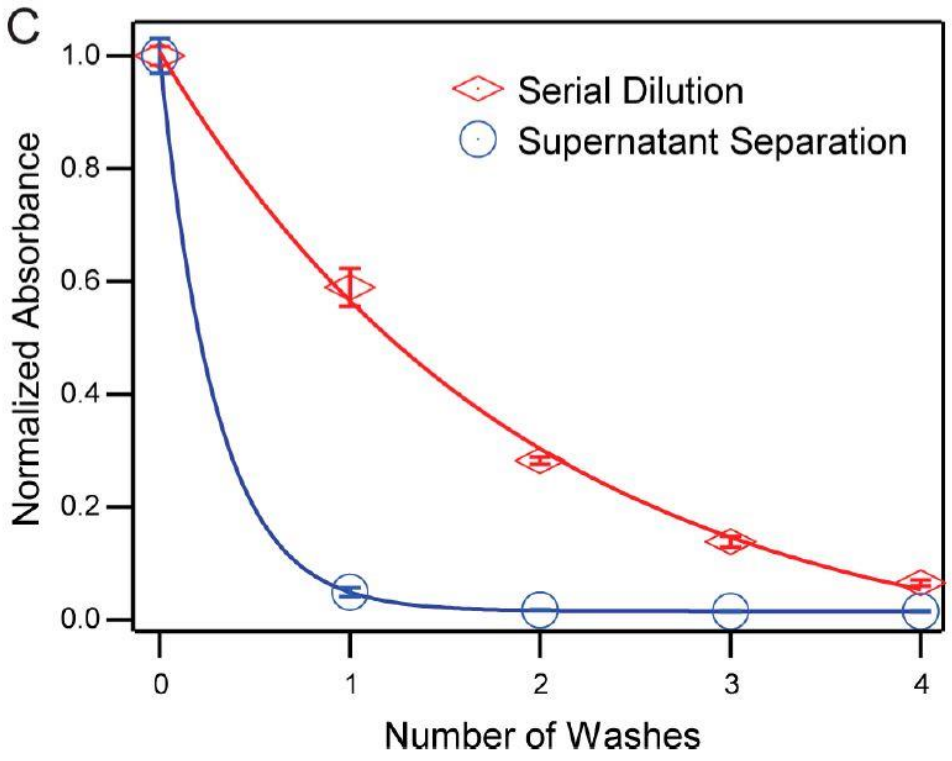

Figure 5.5: Comparison of efficiency of serial dilution vs supernatant separation [29]

Detection is a determining factor of success for testing the DMF device. It mainly consists of using a fluorescent biological marker that binds to the magnetic beads. This marker is then detected via chemiluminescence, using equipment to pick up a fluorescent signal. The intensity of this signal is then correlated with the number of biological markers attached to the beads present in the droplet [29]. Two types of efficiency can then be determined: a washing efficiency, measuring how much unbound reagent is present in the waste droplet, and a retention efficiency, measuring the bead loss during washing protocols. An example of detection performed was via direct fluorescent label on a secondary antibody (FIA) or an enzyme labeled secondary antibody (ELISA). The efficiency of the washing protocol was linked to the amount of Horse Radish Peroxidase (HRP), the label for the magnetic beads (figure 5.6). Its presence was

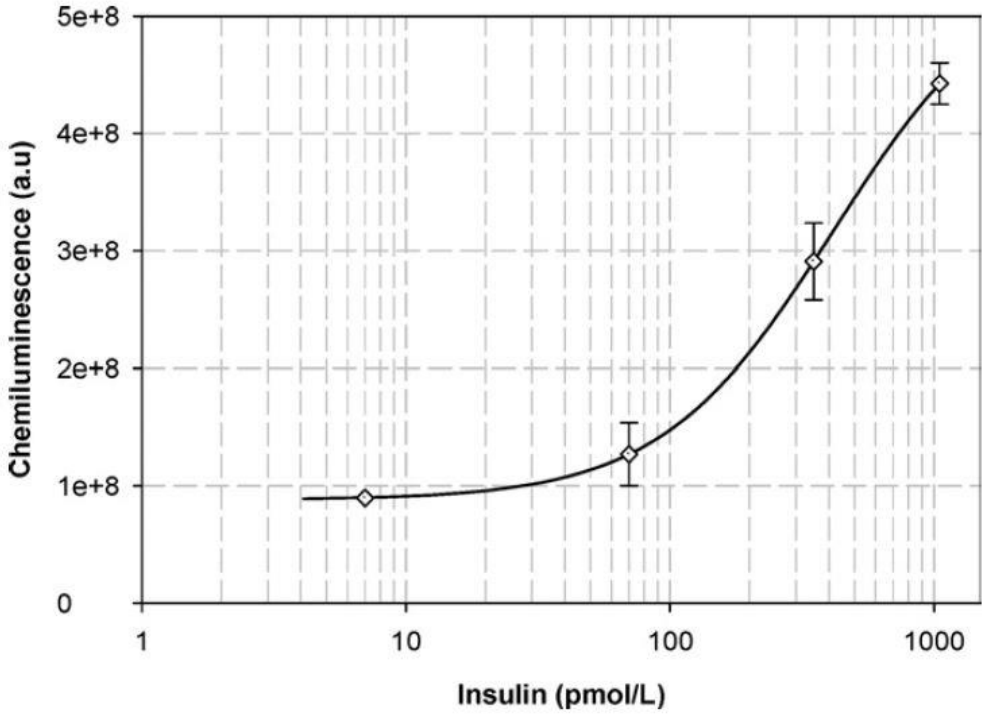

Figure 5.6: Example of detection graph presenting the evolution of concentration of insulin vs chemiluminescence [28]

measured by adding Amplex Ultra red substrate to the supernatant wash droplets, and reading the change in absorbance using a BioTEK Synergy plate reader [28].

Anticipating for the next years of research in this area, a tentative detection protocol has been hypothesized. We will be using a fluorescent microscope and fluorescent dye instead of biological markers. After adding the dye, we will be able to measure the intensity of the fluorescent signals emitted. Two signals will be emitted from the device after reaching the dye excitement wavelength: green and red for instance (figure 5.7). Since these lights emit at different wavelengths, we will need two different filters. The red filter on the microscope will allow the evaluation of the washing efficiency while the green filter will help quantify the retention efficiency of the device (hypothetically).

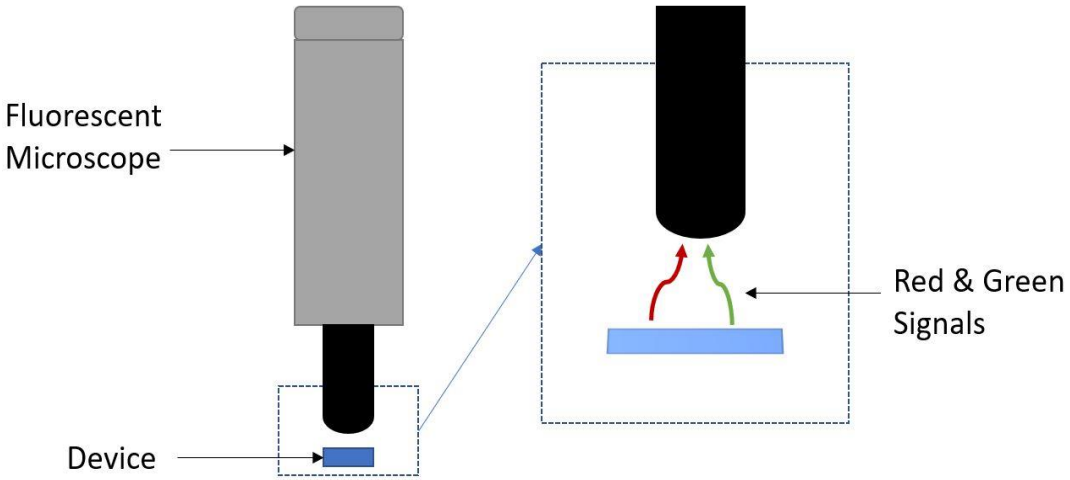

Figure 5.7: Sketch of microscope to measure signals after introducing fluorescent dye

We should be able to plot a graph representing the number of washes vs the ratio of the fluorescent intensity after the wash to the initial intensity (I/I_0) for each of the washing and retention efficiencies. This will then give an idea of the percentage evolution after each wash. We should expect an almost constant retention of beads (green) and an exponential decay-like evolution for the washing efficiency (red) (figure 5.8).

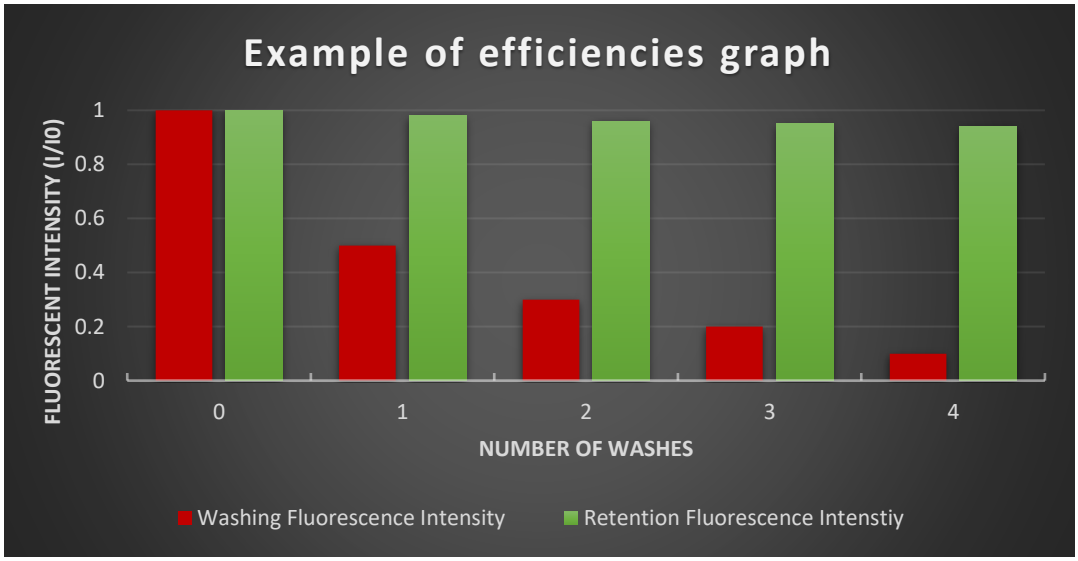

Figure 5.8: Example of efficiencies graph

REFERENCES

[1] W. S. Marshall and R. J. Kaiser, “Recent advances in the high-speed solid phase synthesis of RNA,” *Curr. Opin. Chem. Biol.*, vol. 8, no. 3, pp. 222–229, 2004.

[2] H. W. D. Matthes *et al.*, “Simultaneous rapid chemical synthesis of over one hundred oligonucleotides on a microscale,” *Embo J.*, vol. 3, no. 4, pp. 801–805, 1984.

[3] M. Bevan, M. Lane, and C. Cb, “Nucleic Acids Research,” *Nucleic Acids Res.*, vol. 37, no. Database, pp. ii–ii, 2008.

[4] M. Caruthers, “Gene synthesis machines: DNA chemistry and its uses,” *Science (80-.).*, vol. 230, no. 4723, pp. 281–285, 1985.

[5] R. Sista *et al.*, “Development of a digital microfluidic platform for point of care testing,” *Lab Chip*, vol. 8, no. 12, p. 2091, 2008.

[6] S. H. Weisbrod and A. Marx, “A nucleoside triphosphate for site-specific labelling of DNA by the Staudinger ligation,” *Chem. Commun.*, no. 18, pp. 1828–1830, 2007.

[7] D. Chatterjee, B. Hetayothin, A. R. Wheeler, D. J. King, and R. L. Garrell, “Droplet-based microfluidics with nonaqueous solvents and solutions,” *Lab Chip*, vol. 6, no. 2, pp. 199–206, 2006.

[8] I. D. Technologies, “Chemical Synthesis and Purification of Oligonucleotides,” 2011.

[9] E. R. F. Welch, Y. Lin, A. Madison, and R. B. Fair, “Picoliter DNA Sequencing Chemistry on an Electrowetting-based Digital Microfluidic Platform,” vol. 6, no. 2, pp. 1–20, 2012.

[10] O. Morozova and M. A. Marra, “Applications of next-generation sequencing technologies in functional genomics,” *Genomics*, vol. 92, no. 5, pp. 255–264, 2008.

[11] G. McGall, J. Labadie, P. Brock, G. Wallraff, T. Nguyen, and W. Hinsberg, “Light-directed synthesis of high-density oligonucleotide arrays using semiconductor photoresists.,” *Proc. Natl. Acad. Sci. U. S. A.*, vol. 93, no. 24, pp. 13555–13560, 1996.

[12] R. Drmanac *et al.*, “3′ Branch ligation: a novel method to ligate non-complementary DNA to recessed or internal 3′OH ends in DNA or RNA,” *DNA Research*. 2018.

[13] W.-Y. Chang, H.-Y. Chang, D.-J. Yao, Y.-J. Liu, and H.-C. Lin, “DNA ligation of ultramicro volume using an EWOD microfluidic system with coplanar electrodes,” *J. Micromechanics Microengineering*, vol. 18, no. 4, p. 045017, 2008.

[14] P. Mitchell, “Microfluidics — downsizing large-scale biology To what extent has microfluidics technology fulfilled life science researchers ’ expectations of creating a viable ‘lab-on-a-chip,’” *Nat. Biotechnol.*, vol. 19, pp. 717–721, 2001.

[15] F. P. Documents and O. Publications, “(12) United States Patent “ K,” vol. 1, no. 12, 2001.

[16] G. M. Walker and D. J. Beebe, “A passive pumping method for microfluidic devices,” *Lab Chip*, vol. 2, no. 3, p. 131, 2002.

[17] T. Geng *et al.*, “Multimodal microchannel and nanowell-based microfluidic platforms for bioimaging,” *IEEE Int. Conf. Nano/Molecular Med. Eng. NANOMED*, pp. 155–158, 2017.

[18] P. Gravesen, “Microfluidics-a review,” *J. Micromechanics Microengineering*, vol. 3, no. 4, pp. 168–182, 1993.

[19] C. D. Chin *et al.*, “Microfluidics-based diagnostics of infectious diseases in the developing world,” *Nat. Med.*, vol. 17, p. 1015, Jul. 2011.

[20] S. M. Berry, L. J. MacCoux, and D. J. Beebe, “Streamlining immunoassays with immiscible filtrations assisted by surface tension,” *Anal. Chem.*, vol. 84, no. 13, pp. 5518–5523, 2012.

[21] M. G. Pollack, R. B. Fair, E. J. Shaughnessy, and G. A. Ybarra, “ELECTROWETTING-BASED MICROACTUATION OF DROPLETS FOR DIGITAL MICROFLUIDICS,” *Biogr. An Interdiscip. Q.*, 2001.

[22] S.-Y. Teh, R. Lin, L.-H. Hung, and A. P. Lee, “Droplet microfluidics,” *Lab Chip*, vol. 8, no. 2, pp. 198–220, 2008.

[23] R. B. Fair, *Digital microfluidics: Is a true lab-on-a-chip possible?*, vol. 3, no. 3. 2007.

[24] T. S. Hwa, “Droplet-Based Microfluidics,” 2010.

[25] H. R. Nejad, O. Z. Chowdhury, M. D. Buat, and M. Hoorfar, “Characterization of the geometry of negative dielectrophoresis traps for particle immobilization in digital microfluidic platforms.,” *Lab Chip*, vol. 13, no. 9, pp. 1823–1830, 2013.

[26] K. Choi, A. H. C. Ng, R. Fobel, and A. R. Wheeler, “Digital Microfluidics,” *Annu. Rev. Anal. Chem.*, vol. 5, no. 1, pp. 413–440, 2012.

[27] S. C. C. Shih *et al.*, “A droplet-to-digital (D2D) microfluidic device for single cell assays,” *Lab Chip*, vol. 15, no. 1, pp. 225–236, 2015.

[28] R. S. Sista, A. E. Eckhardt, V. Srinivasan, M. G. Pollack, S. Palanki, and V. K. Pamula, “Heterogeneous immunoassays using magnetic beads on a digital microfluidic platform,” *Lab Chip*, vol. 8, no. 12, p. 2188, 2008.

[29] A. H. C. Ng *et al.*, “Digital Micro fluidic Magnetic Separation for Particle-Based Immunoassays,” *Anal. Chem.*, vol. 84, pp. 8805–12, 2012.

[30] C. Dixon, A. H. C. Ng, R. Fobel, M. B. Miltenburg, and A. R. Wheeler, “An inkjet printed, roll-coated digital microfluidic device for inexpensive, miniaturized diagnostic assays,” *Lab Chip*, vol. 16, no. 23, pp. 4560–4568, 2016.

[31] X. Li, D. R. Ballerini, and W. Shen, “A perspective on paper-based microfluidics: Current status and future trends,” *Biomicrofluidics*, vol. 6, no. 1, 2012.

[32] K. A. Bernetski, C. T. Burkhart, K. L. Maki, and M. J. Schertzer, “Characterization of electrowetting, contact angle hysteresis, and adhesion on digital microfluidic devices with inkjet-printed electrodes,” *Microfluid. Nanofluidics*, vol. 22, no. 9, pp. 1–10, 2018.

[33] V. Jain, T. P. Raj, R. Deshmukh, and R. Patrikar, “Design, fabrication and characterization of low cost printed circuit board based EWOD device for digital microfluidics applications,” *Microsyst. Technol.*, vol. 23, no. 2, pp. 389–397, 2017.

[34] Sung Kwon Cho, Hyejin Moon, and Chang-Jin Kim, “Creating, transporting, cutting, and merging liquid droplets by electrowetting-based actuation for digital microfluidic circuits,” *J. Microelectromechanical Syst.*, vol. 12, no. 1, pp. 70–80, 2003.

[35] N. Y. J. B. Nikapitiya, S. M. You, and H. Moon, “Droplet dispensing and splitting by electrowetting on dielectric digital microfluidics,” *Proc. IEEE Int. Conf. Micro Electro Mech. Syst.*, pp. 955–958, 2014.

[36] M. A. Cleary *et al.*, “Production of complex nucleic acid libraries using highly parallel in situ oligonucleotide synthesis,” *Nat. Methods*, vol. 1, no. 3, pp. 241–248, 2004.

[37] M. T. Guo, A. Rotem, J. a. Heyman, and D. a. Weitz, “Droplet microfluidics for high-throughput biological assays,” *Lab Chip*, vol. 12, no. 12, p. 2146, 2012.

[38] C. Yi, C. W. Li, S. Ji, and M. Yang, “Microfluidics technology for manipulation and analysis of biological cells,” *Anal. Chim. Acta*, vol. 560, no. 1–2, pp. 1–23, 2006.

[39] M. J. Schertzer, R. Ben-Mrad, and P. E. Sullivan, “Mechanical filtration of particles in electrowetting on dielectric devices,” *J. Microelectromechanical Syst.*, vol. 20, no. 4, pp. 1010–1015, 2011.

[40] ATDBIO, “Solid-phase oligonucleotide synthesis.” [Online]. Available: https://www.atdbio.com/content/17/Solid-phase-oligonucleotide-synthesis#Advantages-of-solid-phase-synthesis. [Accessed: 29-Jan-2018].

[41] “DNA ligation — Science Learning Hub.” [Online]. Available: https://www.sciencelearn.org.nz/resources/2034-dna-ligation. [Accessed: 02-Apr-2019].

APPENDIX A

Supplemental Labview code employed to operate the DMF device:

(1) create/dispense droplets
(2) moving droplets
(3) dispensing and moving from two reservoirs

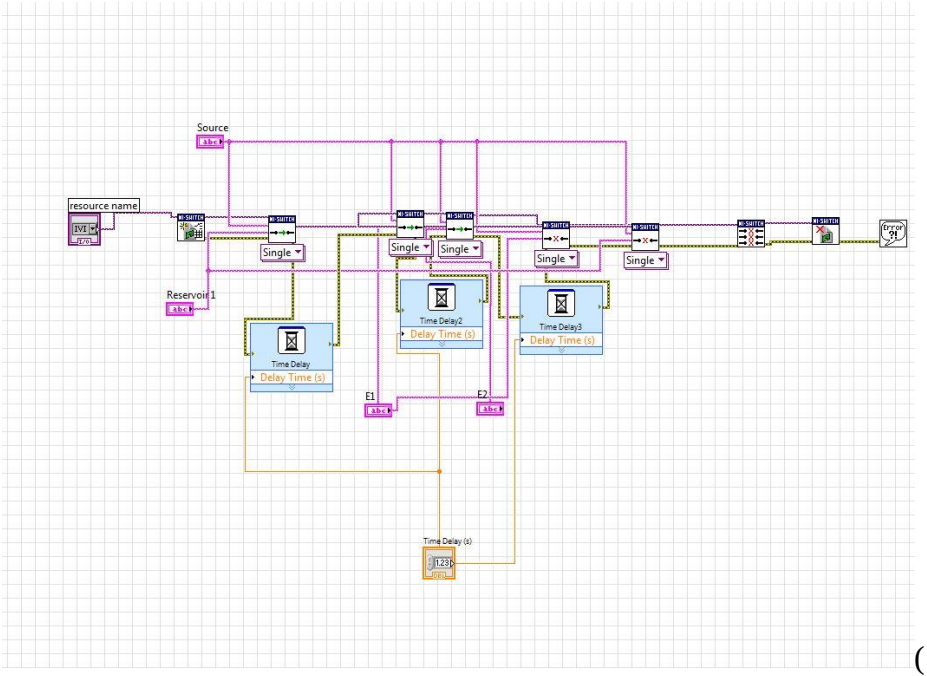

(1)

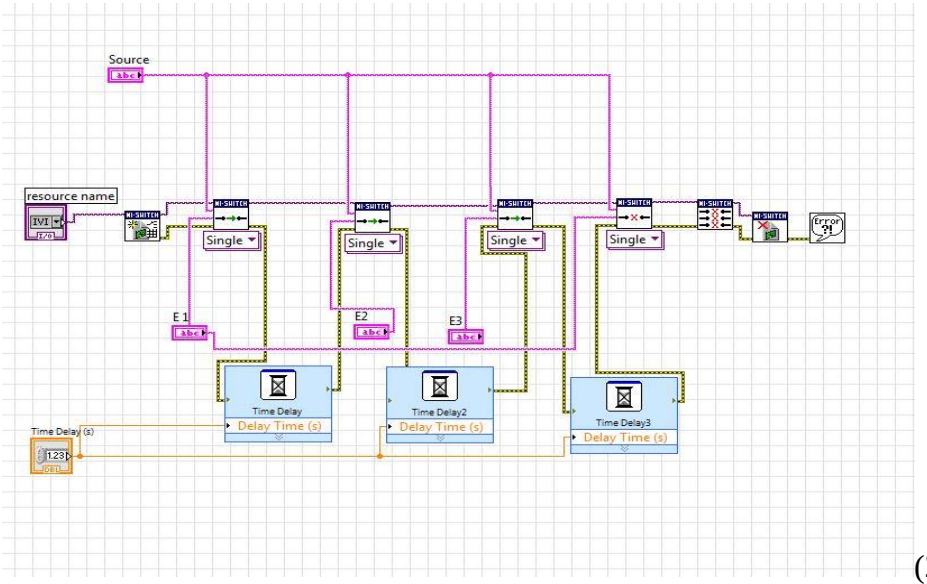

(2)

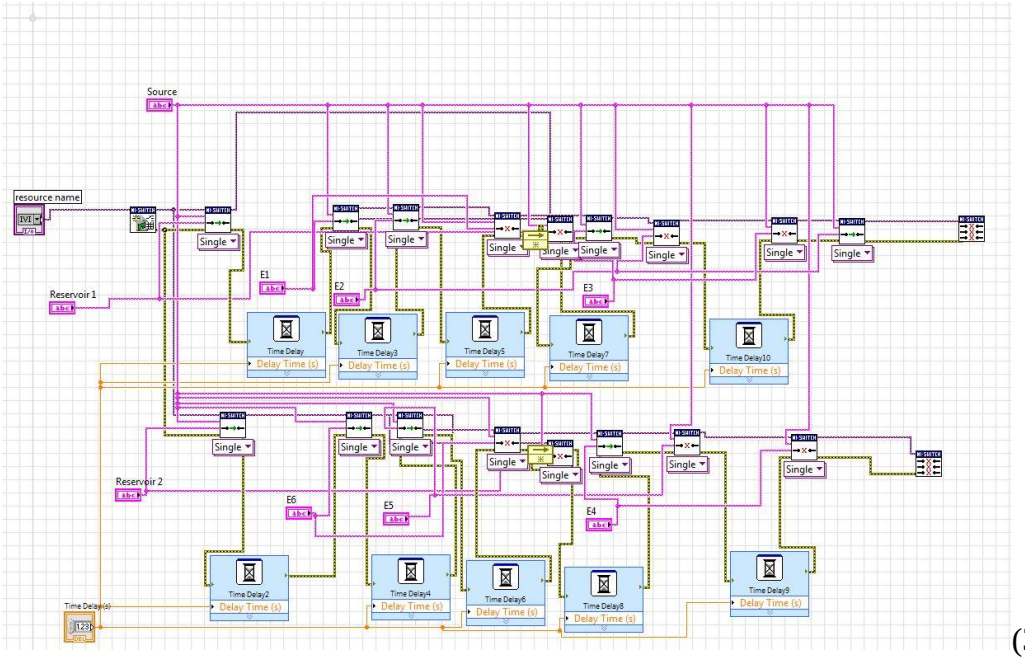
Source
resource name
Reservoir 1
Reservoir 2
E1
E2
E3
E4
E5
E6
Single
Time Delay
Time Delay2
Time Delay3
Time Delay4
Time Delay5
Time Delay6
Time Delay7
Time Delay8
Time Delay9
Time Delay10
Delay Time (s)
Time Delay(s)

(3)